STANFORD GEOTHERMAL PROGRAM
STANFORD UNIVERSITY

Stanford Geothermal Program
Interdisciplinary Research in
Engineering and Earth Sciences
STANFORD UNIVERSITY
Stanford, California

SGP-TR-75

USER'S MANUAL FOR THE ONE-DIMENSIONAL LINEAR HEAT SWEEP MODEL

By

A. Hunsbedt
S. T. Lam
P. Kruger

April, 1984

Financial support was provided through the Stanford Geothermal Program under Department of Energy Contract No. DE-AT03-80SF11459 and by the Department of Civil Engineering, Stanford University.

ABSTRACT

This manual describes a 1-D linear heat sweep model for estimating energy recovery from fractured geothermal reservoirs based on early estimates of the geological description and heat transfer properties of the formation. The manual describes the mathematical basis for the heat sweep model and its use is illustrated with the analysis of a controlled experiment conducted in the Stanford Geothermal Program's large physical model of a fractured-rock hydrothermal reservoir. The experiment, involving known geometry and heat transfer properties, allows evaluation of the model's capabilities, accuracy, and limitations. The manual also presents an analysis of a hypothetical field problem to illustrate the applicability of the model for making early estimates of energy extraction potential in newly developing geothermal fields.

Further development of the model is underway. Enhancement of the modal from one-dimensional linear sweep to one-dimensional radial sweep will expand its application for early estimate of energy extraction to more complex geothermal fields. Other improvements to the model may involve inclusion of variable water production/recharge rate and more detailed estimate of the heat transfer from the surrounding rock formation. The manual will be revised as these enhancements are achieved.

TABLE OF CONTENTS

LIST OF FIGURES

LIST OF TABLES

1. INTRODUCTION

Since 1972, the Stanford Geothermal Program has had a continuous objective of investigating means of enhanced energy recovery from geothermal resources. One of the key objectives is the technical basis for early assessment of the amount of extractable energy from hydrothermal resources under various production strategies, The 1-D Linear Heat Sweep Model has been developed from a physical model of a fractured rock, hydrothermal reservoir to estimate the potential for energy extraction based on limited amounts oh geologic and thermodynamic data.

The potential for energy recovery from hydrothermal reservoirs was examined by Ramey, Kruger, and Raghavan (1973) for hypothetical steam and hot water reservoirs similar in size and properties. The data in Table 1-1 were calculated for geothermal reservoirs at an initial temperature of 260°C, porosity of 25 percent over a reservoir volume 1230 m^3 in extent, with steam enthalpy of 2.33 MJ/kg for a useful life based on pressure decline from 4.7 MPa (at 260°C) to an abandonment pressure of 0.7 MPa (at 164°C). The data show that only 6 percent of the available energy in the steam reservoir is in the geofluid, while 94 percent is in the formation rock. It is apparent that a method of "sweeping" the heat in the rock by recycling of cooler water through the reservoir could significantly enhance energy recovery.

The development of the 1-D Linear Heat Sweep Model has been accomplished in three phases. The first phase! involved a lumped-parameter analysis of energy recovery using three non-isothermal production methods (Hunsbedt, Kruger, and London, 1978): (1) pressure reduction with in-place boiling; (2) reservoir sweep with injection of cold water; and (3) steam drive with pressurized fluid production. Results of these studies are summarized in Table 1-2. From a thermodynamic point of view, it appears that reservoit

sweep with cycled cold water (under carefully controlled conditions to avoid short-circuiting and mineral deposition) could effectively enhance overall energy extraction.

The second phase involved development of a heat transfer model for a collection of irregular-shaped rocks with arbitrary size distribution. The efforts of Kuo, Kruger, and Brigham **(1976)** resulted in adequate correlations of shape factors with thermodynamic properties of single irregular-shaped rock blocks. The work by Iregui, Hunsbedt, Kruger, and London **(1979)** extended the correlations to assemblies of fractured blocks. The result was a one-dimensional model of a hydrothermal, fractured rock system under cold water injection heat sweep based on a single spherical rock block of "effective radius".

The third phase of the development has been based on experimental verification of the ability of *a* 1-D heat sweep model to predict energy recovery from a rock loading of known, regular geometric shape and thermal properties, The model is based on input knowledge of the volumetric distribution of rock blocks and the rock heat transfer parameters. The experimental parameters of the model are the "number of heat transfer units" and the initial distributian of energy stored in the water and rock. The "number of heat transfer units" parameter is determined by the estimated fluid residence time and the time constant for the rock block (a function of equivalent rock radius, thermal diffusivity, and Biot number). AS the most significant parameter in the 1-D Heat Sweep Model, it indicates the degree to which energy extraction from potential hydrothermal reservoirs is heat transfer limited or water supply limited.

This manual describes the mathematical basis for the model and provides a working means for its use through analysis of two sample problems. The model

is intended for early use in analysis of new geothermal reservoirs to test evaluations of geologic estimations of rock type and fracture distribution. Early application of the model to real reservoirs should provide feedback as to current model limitations and a basis for improvements. Further development of the model is expected to enhance its applicability in the early analyses of more complex geothermal reservoirs.

Table 1-1

RELATIVE RECOVERY FROM HYDROTHERMAL RESERVOIRS*

	Steam Reservoir		Hot Water Reservoir	
	Rock	Fluid	Rock	Fluid
Reservoir Mass (kg)	2.45×10^6	7,330	2.45×10^6	242,100
Abandonment Content (kg)	--	885	--	28,260
Production (kg)	--	6,445	--	213,840
as Steam	--	6,445	--	168,740
as Water	--	0	--	45,100
Available Energy (GJ)	246	16	246	106
Recovery of Fluid Mass (%)	--	87.9	--	88.3
Recovery of Available Energy (%)	--	6.1	--	99.1

* for a hypothetical reservoir of 260°C temperature, 25% porosity, $1230 m^3$ volume, 2.33 MJ/kg steam enthalpy, and abandonment pressure of 0.69 MPa (at 164°C). Adapted from Ramey, Kruger, Raghavan (1973).

Table 1-2

RESULTS OF EARLY HEAT EXTRACTION EXPERIMENTS

Production Method	Specific Energy Extraction (kJ/kg)	Energy Extraction Fraction (%)
In-Place Boiling	83 - 116	75 - 100
Sweep	145 - 175	80 - 86*
Steam Drive	21	22 - 27

* Based on steady-state water injection temperature. Others based on saturation temperature at final pressure. Adapted from Hunsbedt, Kruger, and London, (1977).

2. MATHEMATICAL MODEL

The one-dimensional linear sweep model is designed to calculate water and rock matrix temperature distributions in a fractured hydrothermal reservoir as functions of distance from the injection point and time of production.

2.1 Geometry and Assumptions

The reservoir geometry of the 1-D heat sweep model is given in Figure 2-1. Cold water at temperature T_{in} is injected through a line of wells at point A and produced at the same rate through a line of wells at point B. The distance between the injection and production wells is L, and the cross-sectional area of the reservoir is S. The initial temperature of both the reservoir water and rock is T_1 everywhere in the reservoir. The cold water injection temperature T_{in} may be constant or decrease exponentially from the initial reservoir temperature to a lower constant value.

The reservoir rock consists of rock blocks of various sizes and of irregular shape. The intrinsic permeability of the rock blocks is essentially zero while the permeability of the reservoir is considered to be essentially infinite. Based on the work of Kuo et al. (1976), it is assumed that the rock formation is thermally characterized by a single effective block size of radius $R_{e,c}$. The rock block size distribution is assumed to be uniform in the reservoir. The fracture porosity and flow velocity in the reservoir are assumed to be constant over the cross-sectional area (S), and do not vary with distance (L) between the injection and production wells.

Heat transfer per unit reservoir length and per unit time q' along the direction of flow is assumed to be constant in time and space. The sign convention used is that q' is positive when heat flow is from the surrounding rock formation to the reservoir rock formation. Two-dimensional effects

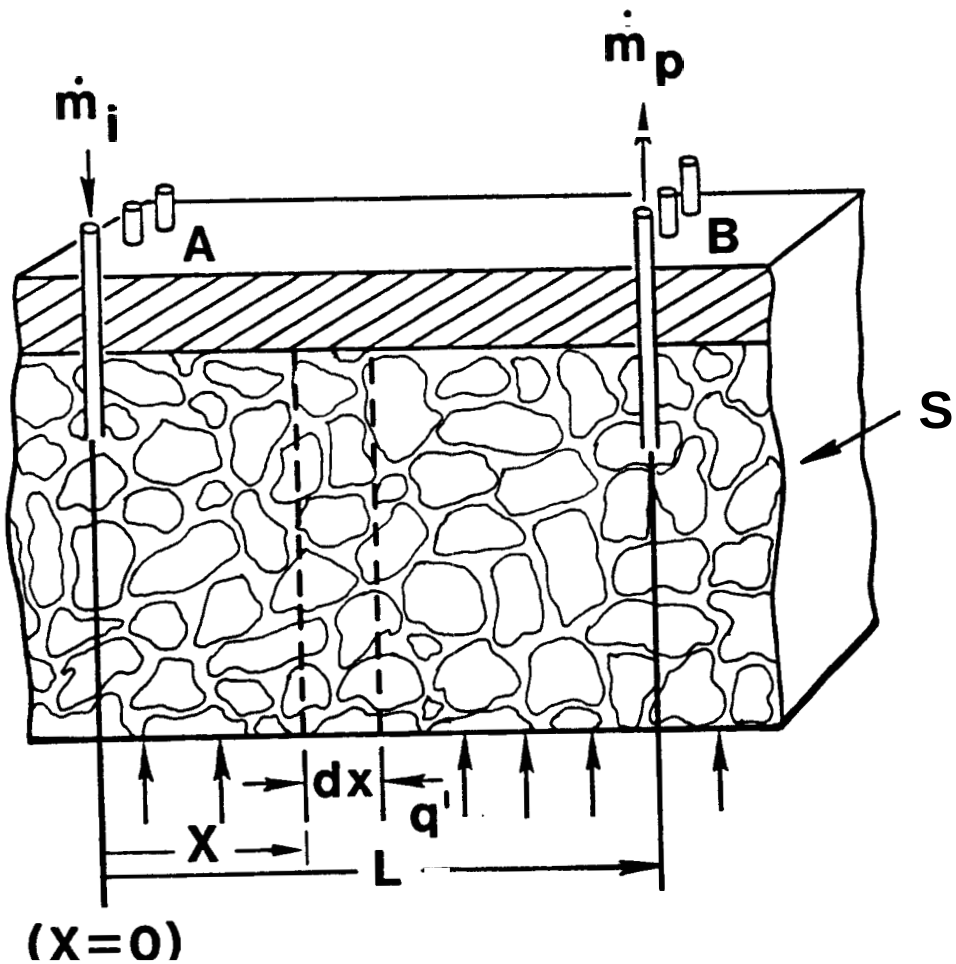

Fig. 2–1: 1-D Linear Heat Sweep **Model** Geometry

such as gravity segregation of cold water to the bottom layers of the reservoir, and axial heat conduction are neglected. Physical and thermal properties of both water and rock are assumed to be constant.

The 1-D heat sweep model takes into account the temperature gradient inside large rock fragments produced by long path lengths for heat conduction and low rock thermal conductivity when cold water flows along the rock surfaces. Previous analyses performed by Schuman (1929) and Löf and Hawley (1948) for air flowing through a rock matrix neglected the thermal resistance inside the rock itself while considering only the surface resistance. This assumption may be correct for air flow. It is not acceptable for water because the surface resistance is usually very low compared to the internal rock thermal resistance, indicated by a high Biot number.

2.2 Governing Equations

A thin element of the reservoir (shown in Figure 2-1) of thickness dx and cross-sectional area S is the representative volume in deriving the governing equation for the reservoir water temperature. An energy balance on this element results in the following partial differential equation for the water temperature

$$\frac{\partial T_f}{\partial x} + \frac{\phi}{u_f}\frac{\partial T_f}{\partial t} + \frac{(1-\phi)}{u_f}\frac{\rho_r C_r}{\rho_f C_f}\frac{\partial \overline{T}_r}{\partial t} = \frac{q'}{\rho_f u_f S C_f} \qquad (2\text{-}1a)$$

The initial and boundary conditions, respectively, are

$$T_f(x,0) = T_1 \qquad (2\text{-}1b)$$

$$T_f(0,t) = (T_1 - T_{in})e^{\beta t} + T_{in} \qquad (2\text{-}1c)$$

Explanation of the symbols used in the manual are compiled in the nomenclature section. The parameter β, referred to as the recharge temperature parameter is selected by the user to give the desired inlet condition. Referring to Eq. (2-1c), it is noted that $\beta = -\infty$ hr^{-1} gives a step change in the water inlet temperature while a finite and negative value of β gives an exponentially decreasing inlet temperature. For well defined situations, such as flow of recharge water down an injection well, it is possible to estimate the value of β using the procedure developed by Ramey (1962). In other cases, however, the flow path of surface water recharge in a geothermal reservoir may be undefined, and $\beta = -\infty$ hr^{-1} is recommended when β cannot be estimated.

An energy balance on the rock fragments within the differential element gives for the average rock temperature

$$\frac{\partial \bar{T}_r}{\partial t} = \frac{T_f - \bar{T}_r}{\frac{R_{e,c}^2}{3\alpha}\left(\frac{l_{cond}}{R_{e,c}} + \frac{1}{N_{Bi}}\right)} \qquad (2\text{-}2a)$$

The conduction path length l_{cond} is used to represent the internal rock thermal resistance. The ratio $l_{cond}/R_{e,c}$ was determined to be approximately 0.2 for spherical shapes (Hunsbedt et al. (1977) and Iregui et al. (1979)). The time constant for the rock fragments of radius $R_{e,c}$ is defined as

$$\tau = \frac{R_{e,c}^2}{3\alpha}\,(0.2 + 1/N_{Bi}) \qquad (2\text{-}2b)$$

Reference is made to section 2.4.1 for definition of $R_{e,c}$, referred to as the effective rock size of a rock collection. Substituting the time constant into Eq. (2-2a) gives for the rock temperature

$$\frac{\partial \overline{T}_r}{at} = \frac{T_f - \overline{T}_r}{f} \qquad (2\text{-}2c)$$

which is solved with the initial condition

$$\overline{T}_r(x,0) = T_1 \qquad (2\text{-}2d)$$

Equations (2-la) and (2-2c) are a set of coupled partial differential equations, which can be simplified by introducing non-dimensional variables as follows:

Temperature:

$$T_f^* = (T_f(x,t) - T_{in})/(T_1 - T_{in}) \qquad (2\text{-}3a)$$

$$\overline{T}_r^* = (\overline{T}_r(x,t) - T_{in})/(T_1 - T_{in}) \qquad (2\text{-}3b)$$

Space:

$$x^* = x/L \qquad (2\text{-}3c)$$

Time:

$$t^* = t/t_{re} \qquad (2\text{-}3d)$$

Number of Heat Transfer Units Parameter:

$$N_{tu} = t_{re}/\tau \qquad (2\text{-}3e)$$

External Heat Transfer Parameter

$$q^* = q'L/\rho u_f S C_f (T_1 - T_{in}) \qquad (2\text{-}3f)$$

Storage Ratio

$$\gamma = \rho_f C_f \phi / \rho_r C_r (1-\phi) \qquad (2\text{-}3g)$$

Recharge Temperature Parameter

$$\beta^* = \beta t_{re} \qquad (2\text{-}3h)$$

These non-dimensional variables and parameters allow the partial differential equations and boundary/initial conditions to be written as

$$\frac{\partial T_f^*}{\partial x^*} + \frac{\partial T_f^*}{\partial t^*} + \frac{1}{\gamma}\frac{\partial \bar{T}_r^*}{\partial t^*} = q^* \tag{2-4a}$$

$$T_f^*(x^*,0) = 1 \tag{2-4b}$$

$$T_f^*(0,t^*) = e^{\beta^* t^*} \tag{2-4c}$$

and

$$\frac{\partial \bar{T}_r^*}{\partial t^*} = N_{tu}(T_f^* - \bar{T}_r^*) \tag{2-4d}$$

$$\bar{T}_r^*(x^*,0) = 1 \tag{2-4e}$$

2.3 Solution Procedure

An analytical solution to the governing equations is not available. However, a solution has been obtained by numerical integration using finite difference techniques. The technique adopted for the model involves transforming into the Laplace space combined with a numerical inversion algorithm.

The Laplace transform of Eqs. (2-4a), (2-4c), and (2-4d) with the initial conditions given by Eqs. (2-4b) and (2-4e) results in the following set of equations

$$\frac{\partial \hat{T}_f^*}{\partial x^*} + s\,\hat{T}_f^* - 1 + \frac{1}{\gamma}[s\,\hat{\bar{T}}_r^* - 1] = q^*/s \tag{2-5a}$$

$$s\,\hat{\bar{T}}_r^* - 1 = N_{tu}(\hat{T}_f^* - \hat{\bar{T}}_r^*) \tag{2-5b}$$

with boundary condition

$$\hat{T}_f^*(0,s) = 1/(s - \beta^*) \qquad (2\text{-}5c)$$

Equations (2-5a) and (2-5b) can be solved for $\hat{T}_f^*$ and $\hat{T}_r^*$ to give for the water temperature

$$\frac{d\hat{T}_f^*}{dx^*} + Ks\,\hat{T}_f = \frac{q^*}{s} + K \qquad (2\text{-}6a)$$

where

$$K = 1 + \frac{N_{tu}}{\gamma(s + N_{tu})} \qquad (2\text{-}6b)$$

Integration of Eq. (2-6a) using condition (2-5c) gives the water temperature as

$$T_f^* = \left(\frac{q^*}{Ks^2} + \frac{1}{s}\right) + \left(\frac{1}{s-\beta^*} - \frac{q^*}{Ks^2} - \frac{1}{s}\right) e^{-Ksx^*} \qquad (2\text{-}7a)$$

The corresponding Laplace equation for the rock temperature is

$$\hat{T}_r^* = \frac{1}{s + N_{tu}} + \frac{N_{tu}}{s + N_{tu}}\,\hat{T}_f^* \qquad (2\text{-}7b)$$

Inversion back to real time space gives as the fluid temperature

$$T_f^*(x^*,t^*) = \mathcal{L}^{-1}[T_f^*(x^*,s)] \qquad (2\text{-}8)$$

Inversion of the Laplace transform is performed numerically using the algorithm given by Stehfest (1970):

$$T_f^*(x^*,t^*) = \frac{\ln 2}{t^*} \sum_{i=1}^{M} a_i \hat{T}_f^*\left(x^*, \frac{\ln 2}{t^*} xi\right) \qquad (2\text{-}9a)$$

where the coefficients are given by

$$a_i = (-1)^{M/2+i} \sum_{k=\left(\frac{i+1}{2}\right)}^{\mathrm{Min}(i,M/2)} \frac{k^{(M/2)}(2k)!}{\left(\frac{M}{2}-k\right)!k!(k-1)!(i-k)!(2k-i)!} \qquad (2\text{-}9b)$$

The coefficients are independent of time, so that once the optimum number of terms, M, has been selected, one computation of the coefficients is sufficient for all times. The value of M chosen largely depends on the magnitudes of γ, N_{tu}, and computer accuracy. Results of a study to determine the optimum value of M are presented in section 3.1.5. It was found that, in general, values between 8 and 14 produced good practical results, and that a problem with a higher N_{tu} value usually requires a higher number of terms. Table 2-1 shows these coefficients for values of M between 4 and 12. The Stehfest algorithm solution to Eqs. (2-7a) and (2-7b) can readily be programmed on a hand calculator or microcomputer. A program to perform the calculation is given in Appendix A and a flow diagram of the program in Appendix B. Use of the solution will be demonstrated in later sections.

Table 2-1

COEFFICIENTS FOR INVERSION OF THE LAPLACE TRANSFORM

	Coefficients a_i for given M				
i	4	6	8	10	12
1	-2	1	-0.333...*	0.0833...	-0.01666...
2	26	-49	48.333...	-32.0833...	16.0166...
3	-48	366	-906	1279	-1247
4	24	-858	5,464.666...	-15,623.666...	27,554.333...
5		810	-14,376.666...	84,244.166...	-263,280.833...
6		-270	18,730	-236,957.5	1,324,13847
7			-11,946.666...	375,911.666...	-3,891,705.533...
8			2,986.666...	-340,071.666...	7,053,286.333...
9				164,062.5	-8,005,336.5
10				-32,812.5	5,552,83045
11					-2,155,507.2
12					359,251.2

*... means that the figures continue infinitely.

Recommended for optimum solutions: M = 8 or 10 (M must be an even number).

2.4 Definition of Parameters

The prediction of energy extraction from a fractured geothermal reservoir requires a mathematical heat transfer model to estimate the average rock temperature relative to that of the surrounding fluid. It also requires information on the rock size and shape distributions which are difficult to determine for real geothermal reservoirs. The rock heat transfer model used in the linear heat sweep model was therefore developed in section 2.4.1 for

general size and shape distributions. Evaluation of energy extraction for a variety of assumed reservoir rock parameters can thus be carried out in early stages in the development of a geothermal resource.

2.4.1. Effective Rock Block Radius

The rock heat transfer model was first developed from the work of Kuo, Kruger, and Brigham (1976) for a single rock block of irregular shape by introducing the concepts of a sphericity parameter and effective heat-transfer radius. These concepts were derived on the premise that the thermal behavior of an irregularly shaped body can be approximated as a spherical body having the same surface area to volume ratio. The Kuo sphericity parameter is defined by

$$\Psi_K = \frac{(A/v)_s}{(A/v)_{actual}} = \frac{A_s}{A_{actual}} \qquad (2\text{-}10a)$$

where $A_s = 4\pi R_s^2$ = surface area of a spherical rock with the same volume as the irregularly shaped rock

A_{actual} = actual surface area of the rock block (2-lob)

$$R_s = \left[\frac{3v}{4\pi}\right]^{1/3} = \text{radius of a sphere with the same volume! (v) as the irregularly shaped rock block} \qquad (2\text{-}10c)$$

The sphericity is **less** than unity for all geometric shapes other than the sphere. Equation (2-loa) implies that there is an "effective" sphere radius which will give the correct thermal response for an irregularly shaped rock block. The investigation, carried out by Kuo, Kruger, and Brigham (1976) on a variety of regular and irregularly shaped bodies, showed that such an effective radius could be approximated by

$$R_e = \Psi_K \times R_s \qquad (2\text{-}11)$$

The investigation also showed that surface area to volume ratio is not the only parameter that determines heat: transfer from irregularly shaped bodies, It was expected that a "form factor" which characterizes the effective conduction path length would also have some influence particularly for block shapes where one dimension is much smaller than the other two. This effect is neglected in the linear sweep heat model. In some cases it is possible to approximate the rock blocks shape as flat plates. The theoretical basis for this approach will be considered for inclusion in later versions of this manual.

The heat transfer model for a collection of unequal size rock blocks is based on the earlier observation that the surface area to volume ratio of 8 single rock was the main parameter governing the heat transfer. When this ratio is calculated for the collection of rocks with a given siae distribution, an "effective" single spherical rock having equal surface ares to volume ratio may be used in the heat transfer prediction.

The surface area to volume ratio for the collection is derived using Eqs. (2-10) and (2-11) for each block i in the size distribution and summing for all blocks N as

$$(A/v)_c = 3 \frac{\sum_{i=1}^{N} \frac{R_{s,i}^2}{\Psi_{K,i}}}{\sum_{i=1}^{N} R_{s,i}^3}$$

It is more efficient in the numerical calculation of these sums to considar several size groups N_L each containing approximately equal size block$

rather than each block individually. This is done by introducing the probability density function $p(R_{s,j}) = n_j/N$ where n_j is the number of equal size rock blocks in the j^{th} group. The equivalent size sphere that has this surface area to volume ratio is determined from the ratio $3/R$ for a sphere with radius R. Hence, the equivalent size sphere radius, referred to as the "effective radius" for the collection is defined by

$$R_{e,c} = \overline{\Psi}_K \frac{\sum_{j=1}^{N_L} p(R_{s,j})\, R_{s,j}^3}{\sum_{j=1}^{N_L} p(R_{s,j})\, R_{s,j}^2} \qquad (2\text{-}12)$$

where $\overline{\Psi}_K$ is the average sphericity.

The effective radius used in the heat transfer calculation can be thought of as being the "thermal center" for the collection of rock blocks. It is greater than the mean radius $\overline{R}_s$ and it is skewed by dispersion about the mean toward the larger-sized rock blocks. For example, for a normal distribution with a value of $\sigma_{\overline{R}_s}/\overline{R} = 0.3$, $R_{e,c}$ is 20 percent higher than $\overline{R}_s$ whereas with $\sigma_{\overline{R}_s}/\overline{R}_s = 1$, $R_{e,c}$ is 111 percent higher.

Measurements were carried out for the size distribution of a rock sample from the Piledriver granitic rock chimney* consisting of 360 rock blocks an4 on six "instrumented blocks" with t'hermocouples embedded at the block centers [Iregui et al. (1979)] to determine a typical average value of the sphericity $\overline{\Psi}_K$ for use in Eq. (2-12). The mass, length, breadth, and width (approximate orthogonal axes of the rock) were measured for each block. In addition, the surface area of the six instrumented blocks were determined by a paraffin coating technique used by Kuo, Kruger, and Brigham (1976).

*The Piledriver (61-kt) nuclear explosive was detonated on June 2, 1966 at a depth of 1,500 ft (457m) in a granodiorite formation.

Since it was not practical to measure the surface area of all blocks in the sample, an approximate method of obtaining surface area was found in which the actual area was computed assuming the block shape is an ellipsoid with the measured length, breadth, and width as axes. The resulting sphericity, referred to as the pseudo sphericity Ψ_K^1, was compared for the six instrumented blocks for which the Kuo sphericity Ψ_K [Eq. (2-10a)] based on an independent surface area measurement using the paraffin-coating technique was available. The comparison showed that Ψ_K^1 was within 10 percent of Ψ_K for these rock blocks. The average ratio between the two was found to be

$$\frac{\overline{\Psi_K}}{\Psi_K^1} = 0.97 \pm 0.06 \qquad (2\text{-}13)$$

with a 95 percent confidence level.

The pseudo sphericity was plotted as a function of rock block size. The scatter in the data was found to be significant and a least-squares regression analysis was carried out to determine if a trend in the data could be established. The linear equation representing the "best fit" is

$$\Psi_K^1 = (0.838 + 0.005\ R_s) \pm 0.16 \qquad (2\text{-}14)$$

A coefficient of determination of 0.0195 shows that only 1.95 percent of the variation in Ψ_K^1 is explained by variation in block size, i.e., the sphericity is practically independent of block size for the collection considered, This finding was reinforced by noting that the probability distributions of Ψ_K^1 and the two ratios of measured block axes were found [Iregui et al, (1979)] to be well represented by normal distributions. It is therefore assumed that the sphericity of this rock collection can be represented by a

mean value obtained from Eq. (2-14) and corrected by Eq. (2-13) to give a mean sphericity of

$$\bar{\Psi}_K = 0.97 \times 0.86 = 0.83 \tag{2-15}$$

This value of $\bar{\Psi}_K$ is adopted in the linear heat sweep model for irregularly shaped rock blocks found in geothermal reservoirs.

2.4.2 Energy Extraction Parameters

Parameters used in assessing the degree of energy extraction from the reservoir are defined and calculated by the program listed in Appendix A. A measure of the degree of energy extraction from a rock distribution at time t is defined by

$$F_E = \frac{T_1 - \bar{T}_r}{T_1 - T_f} = 1 - \frac{\bar{T}_r - T_f}{T_1 - T_f} \tag{2-16}$$

This fraction is referred to as the "energy extracted fraction" and measures the amount of energy actually extracted when the rock is cooled from the initial temperature T_1 to the average temperature $\bar{T}_r$ relative to that extracted if the rock is cooled to the surrounding fluid temperature T_f.

The "temperature drop fraction" for the reservoir is calculated from its definition as

$$F_c = \frac{T_1 - \bar{T}_f}{T_1 - T_{in}} = 1 - \int_0^1 T_f^*(x^*, t^*)dx^* \tag{2-17}$$

The temperature drop fraction is a measure of the average reservoir water temperature relative to the injection water temperature at time t.

A measure of total energy extracted at time t to thermal energy stored in rock and water, denoted by the "energy recovery fraction," is given by

$$F_P = \frac{\int_o^{t^*} T_f^*(1,t^*)dt^*}{1 + 1/y} \qquad (2\text{-}18)$$

Finally, the energy extracted fraction for the whole reservoir, as defined earlier for a single rock block (Eq. 2-16) is calculated for a rock block distribution in terms of the two previous parameters for negligible external heat transfer as

$$F_{E,c} = \frac{F_p}{F_c} + \gamma \left[\frac{F_p}{F_c} - 1\right] \qquad (2\text{-}19)$$

This parameter is a measure of average rock temperature relative to average water temperature at time t, i.e., degree of thermal equilibrium between rock and water. For example, $F_{E,c} = 1$ implies complete thermal equilibrium. From Eq. (2-19) it can be seen that the energy recovery fraction for a low porosity ($\lesssim$ 5%) reservoir (in which γ approaches zero) is proportional to the product of $F_{E,c}$ and F_c, or

$$F_p \simeq F_{E,c} \cdot F_c \qquad (2\text{-}20)$$

Equation (2-20) shows that energy recovery from a fractured reservoir can be limited by a small $F_{E,c}$ (heat transfer limitation possibly because of very large rock blocks) or by a small F_c which can occur, for example, if the water flows along preferred paths (fingering effect) in which regions of the reservoir have high water temperatures and correspondingly low rock to water temperature differences to affect the heat transfer from the rock blocks.

3. SAMPLE PROBLEM ANALYSIS

The application of the 1-D linear heat sweep model is illustrated with two sample problem analyses. The first one is the analysis of an experiment performed in the Physical Reservoir Model of the Stanford Geothermal Program and the second problem is a hypothetical field case study. These two problems illustrate the preparation of input data and the interpretation of program output.

3.1 Experimental System Problem

The application of the linear heat sweep model to the physical model experiment illustrates input preparation, interpretation of output data, accuracy of model prediction relative to experimental results, and the basis for choosing the optimum number of terms in the Stehfest algorithm for numerical inversion of the Laplace Transform. A brief description of the experimental system is presented as an aid in interpreting the results.

3.1.1 Physical Model of a Fractured Hydrothermal Reservoir

The SGP physical model has been described in several reports, e.g., Hunsbedt, Kruger and London (1975, 1977, 1978). The main component is a 1.52 m (5 ft) high by 0.61 m (2 ft) diameter insulated pressure vessel. The rock matrix in the reservoir model consists of 30 granite rock blocks of 0.19 x 0.19 m (7.5 x 7.5 inches) square cross section and 24 triangular blocks as shown in Figure 3-1. The blocks are 0.26 m (10.4 inches) high. The average fracture porosity of the reservoir is 17.3 percent.

Vertical channels between blocks are spaced at 0.64 cm (0.25 inch) and horizontal channels between layers are spaced at 0.43 cm (0.17 inch). Significant vertical flow can occur in the relatively large edge channels betweeh the outer rock blocks and the pressure vessel walls.

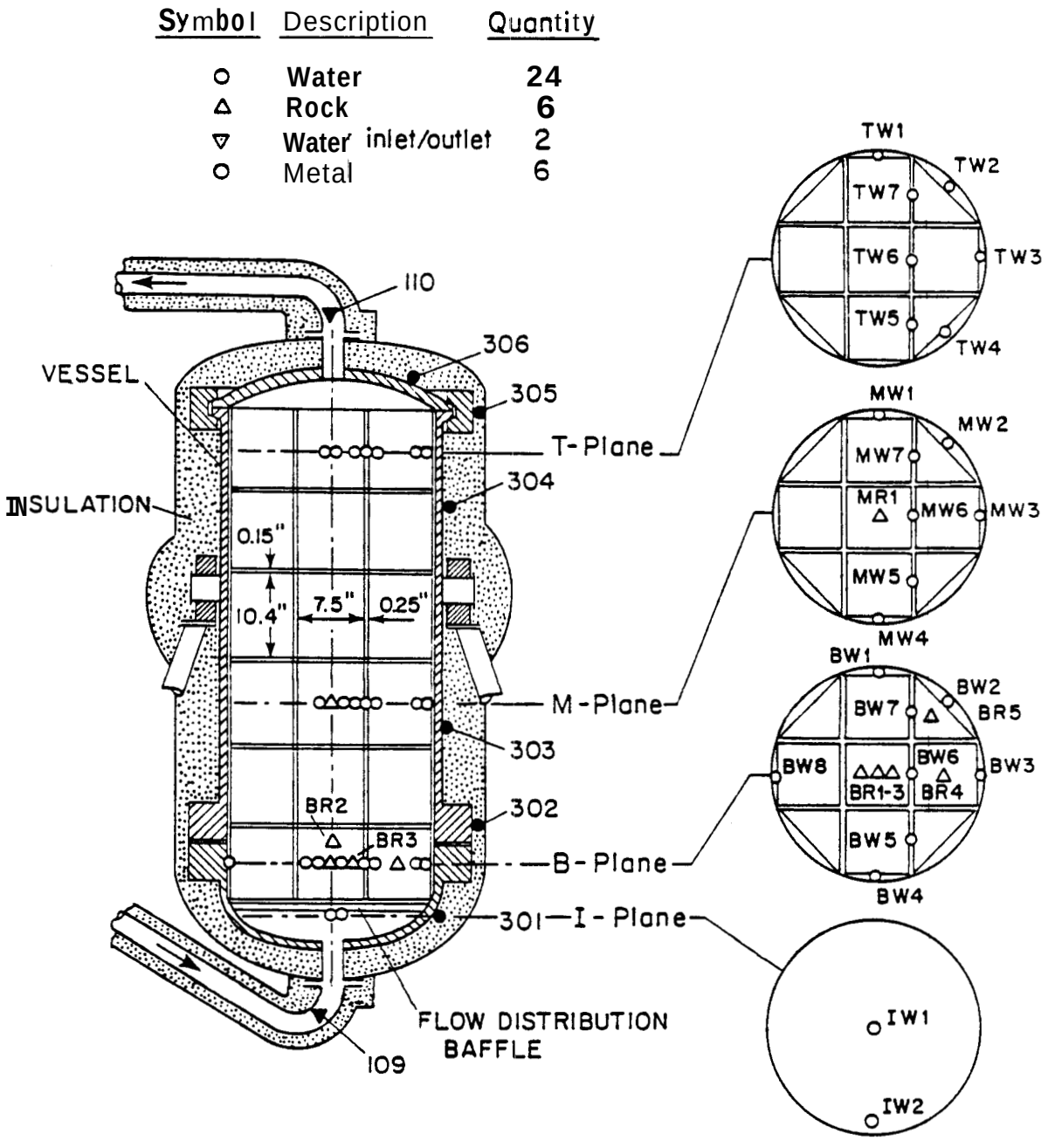

Fig. 3-1: Experimental Rock Matrix Configuration and Thermocouple Locations

Cold water is injected at the bottom of the vessel by a high pressure pump through a flow distribution baffle at the inlet to the rock matrix. System pressure is maintained above saturation throughout the production run by a flow control valve downstream of the vessel outlet. The rock blocks have essentially zero permeability while! the flow in the spaces between the rock blocks is characterized by essentially infinite permeability. Most of the system pressure drop occurs in the flow control valve.

Water temperature is measured at the several locations, as shown in Figure 3–1. Thermocouples are located at the inlet to the vessel, the I-plane just below the baffle, the B-plane half-way up the first rock layer, the M-plane half-way up the third rock layer, the T-plane near the top of the rock matrix, and at the vessel outlet. Rock temperatures are measured at the center of four rock blocks and at two additional locations in the bottom central rock to obtain temperature gradient data at the loction of maximum thermal stress.

An analysis of experiment Run 5–2 was chosen to represent production in a fractured hydrothermal system which results in rapid thermal drawdown of the rock energy. In this experiment, the rock-water-vessel system was heated to a uniform initial temperature by electric strap heaters outside the vessel, Heat extraction was initiated by starting the injection pump and opening the flow control valve. The injection rate was constant during the experiments, Values of the experimental parameters and results of the time-temperature history during production experiment Run 5–2 are summarized in Tables 3–1 and 3–2. Note that the bars in Table 3–2 represent the average value of the several water temperature measurements in each plane (e.g., $\overline{BW}$ is the average water temperature in the B-plane).

Table 3–1

EXPERIMENTAL DATA AND PARAMETERS FOR EXPERIMENT 5–2

Average Reservoir Pressure (MPa)	3.8
Initial Reservoir Temperature (°C)	220
Final Water Temperature at Top (°C)	125
Final Water Temperature at Bottom (°C)	20
Injection Water Temperature (°C)	15.6
Water Xnjection Rate (kg/hr)	227
Production Time (hr)	1.5

Table 3-2

TIME-TEMPERATURE DATA FOR SGP PHYSICAL MODEL EXPERIMENT 5-2

Time (hr)	Temperature (°C) at Thermocouple Location											
	109	110	IW1	IW2	$\overline{BW}$	BR1	BR2	BR4	BR5	$\overline{MW}$	MR1	$\overline{TW}$
0.000	41	222	207	207	220	218	219	218	220	220	221	221
0.083	28	222	102	124	207	218	219	218	219	220	220	220
0.167	24	221	37	47	146	218	219	218	216	219	219	219
0.250	23	221	24	30	96	218	219	218	199	218	219	219
0.333	23	220	24	25	71	213	216	214	168	213	219	218
0.417	20	219	21	24	57	204	206	204	137	198	219	218
0.500	19	218	20	21	47	188	189	189	109	182	218	217
0.667	18	216	19	18	36	147	150	148	71	149	214	213
0.833	17	212	18	17	30	110	114	110	50	120	206	206
1.000	17	203	17	17	25	81	84	81	37	94	188	189
1.167	17	189	17	16	23	59	64	59	29	74	166	169
1.333	16	172	17	16	21	45	49	45	25	59	142	147
1.500	16	152	17	16	20	36	39	36	22	47	117	125

T_∞ = 24.3°C

3.1.2 Input Data Preparation

Preparation of input data for the l-D sweep model is conveniently organized in Table 3-3. Explanation of the various sections of the table, denoted by A, B, C, D, follows.

Table 3-3

LIST OF EXPERIMENTAL PARAMETERS TO LINEAR HEAT SWEEP MODEL
FOR SGP PHYSICAL MODEL PRODUCTION RUN 5-2

A.	Reservoir Conditions	Symbol/Equation	Value	Units
	*Initial Reservoir Temp.	T_1	428	°F
	*Recharge Water Temp.	T_{in}	60	°F
	Recharge Temp. Parameter	β	-23	hr^{-1}
	Production/Recharge Rate	$\dot{m}_p$	501	lb_m/hr
	External Heat Transfer	q'	-1929	Btu/ft hr
B.	Geometry Factors			
	*Reservoir Porosity	ϕ	0.173	dim. less
	Reservoir Cross-sectional Area	S	3.27	ft^2
	Reservoir Length	L	5.06	ft
	Effective Rock Radius	$R_{e,c}$	0.284	ft
C.	Physical Properties			
	Mean Water Density	ρ_f	59.0	$lb_m/ft3$
	Mean Rock Density	ρ_r	167.0	$lb_m/ft3$
	Mean Water Specific Heat	C_f	1.011	$Btu/lb_m°F$
	Mean Rock Specific Heat	C_r	0.218	$Btu/lb_m°F$
	Rock Surface Heat Trans. Coef.	h	300	$Btu/hr°F' ft^2$
	Rock Thermal Conductivity	k	1.4	Btu/hr°F ft
	Rock Thermal Diffusivity	a	0.0385	ft^2/hr
	Steel Vessel "Density"	ρ_m	206.8	$lb_m/ft3$
	Steel Vessel Specific Heat	C_m	0.117	Btu/lb_m

D. Derived Quantities

Rock Capacitance Ratio	$C_r^* = \rho_r C_r / \rho_f C_f$	0.610	dim. less
Steel Capacitance Ratio	$C_m^* = \rho_m C_m / \rho_f C_f$	*0.406*	dim. less
*Combined Rock/Steel Cap. Ratio	$C^* = C_r^* + C_m^*$	1.016	dim. less
Modified Storage Ratio	$\gamma = \phi / C^*(1-\phi)$	0.206	dim. less
Superficial Flow Velocity	$u_f = \dot{m}_p / \rho_f S$	2.597	ft/hr
Pore Flow Velocity	$w = u_f / \phi$	15.01	ft/hr
Water Residence Time	$t_{re} = L/w$	*0.337*	hr
Rock Biot Number	$N_{Bi} = hR_{e,c}/k$	*60.93*	dim. less
Effective Rock Time Constant	$\tau = \frac{R_{e,c}^2}{3a}(0.2+1/N_{Bi})$	0.152	hr
*Recharge Temperature Parameter	$\beta^* = \beta t_{re}$	*-7.9*	dim. less
*No. of Heat Transfer Units	$N_{tu} = t_{re}/\tau$	2.22	dim. less
*External Heat Trans. Param.	$q^* = q'L/\dot{m}_p C_f (T_1 - T_{in})$	-0.0524	dim. less

*starred quantities are inputs to the program

A. Reservoir Conditions

The initial reservoir temperature T_1 is an average of the rock and water temperatures measured prior to initiating production/recharge. The recharge water temperature T_{in} is the steady state temperature attained by the recharge water. This temperature is reached in a period of time that depends on the thermal response characteristics of the physical model in the inlet region. The recharge temperature parameter β^* defined in section 2.2 is used to characterize the thermal response of the system at the inlet loca-

tion. The value of -7.9 given in Table 3-3 was obtained by fitting approximately an exponential curve to the water temperatures measured just below the inlet baffle (T/C's IW1 and IW2 in Figure 3-1) as given in Table 3-2. In a geothermal reservoir, β^* is a parameter the value of which has to be assumed or determined from field data or analysis as indicated in section 2.2. A value of $\beta^* = -\infty$ can be chosen in the absence of more specific information for a geothermal reservoir.

The production/recharge rate m_p is the average rate, measured gravimetrically, at which water is produced during the experiment. The production rate in experiment Run 5-2 was constant at 501 lb_m/hr. The recharge rate is assumed to be equal to the production rate. Thus, small changes in mas8 storage in the vessel as a result of water density changes are not accounted for.

The value given for the external heat transfer parameter q' represents the average amount of heat transfer per foot of reservoir length and per unit time during the experiment. A positive value of q' indicates heat addition to the system while a negative value indicates a heat loss. The value in Table 3-3 was derived from measured vessel temperature data, measured ambient air temperature, and an overall heat: loss coefficient established from earlier cooldown experiments conducted for that purpose. A value of zero should be used in the case of nearly adiabatic reservoir surroundings or in the absence of more specific knowledge for a hydrothermal reservoir.

B. Geometry Factors

The porosity ϕ of the system was calculated from the rock block siae data and the vessel geometry. The cross-sectional area of the vessel S is calculated from the measured inner diameter,

The reservoir length L is the average distance between injection and production levels in the physical model, taken as the length between the top of the flow baffle at the bottom to the top of the upper flange face of the vessel.

Calculation of the effective rock radius $R_{e,c}$ is perhaps the most difficult task for real reservoirs. The calculation procedure for the experimental system is relatively simple as illustrated here.

The arrangement of the 30 rock blocks with square cross-sections and 24 blocks with triangular cross-sections is illustrated in Figure 3-1. The equivalent sphere radius for these two groups and their sphericity were calculated using the rock geometry data and Eqs. (2-10c) and (2-10a):

Block Geometry	Number	Equivalent Sphere Radius (Inches)	Sphericity Ψ_K
Square	30	5.12	0.799
Triangular	24	4.06	0.593

These data are represented as a probability distribution in Figure 3-2. The ordinate represents the number frequency obtained by dividing the number of blocks of each shape (or group) by 54, the total number of blocks. The effective block radius is calculated from Eq. (2-12) for $N_L = 2$ (two groups). Since the sphericity for each group is known, the sphericity factor Ψ_K is kept inside the summation sign in Eq. (2-12). The calculation of sums required for the effective rock radius calculation is given in Table 3-4.

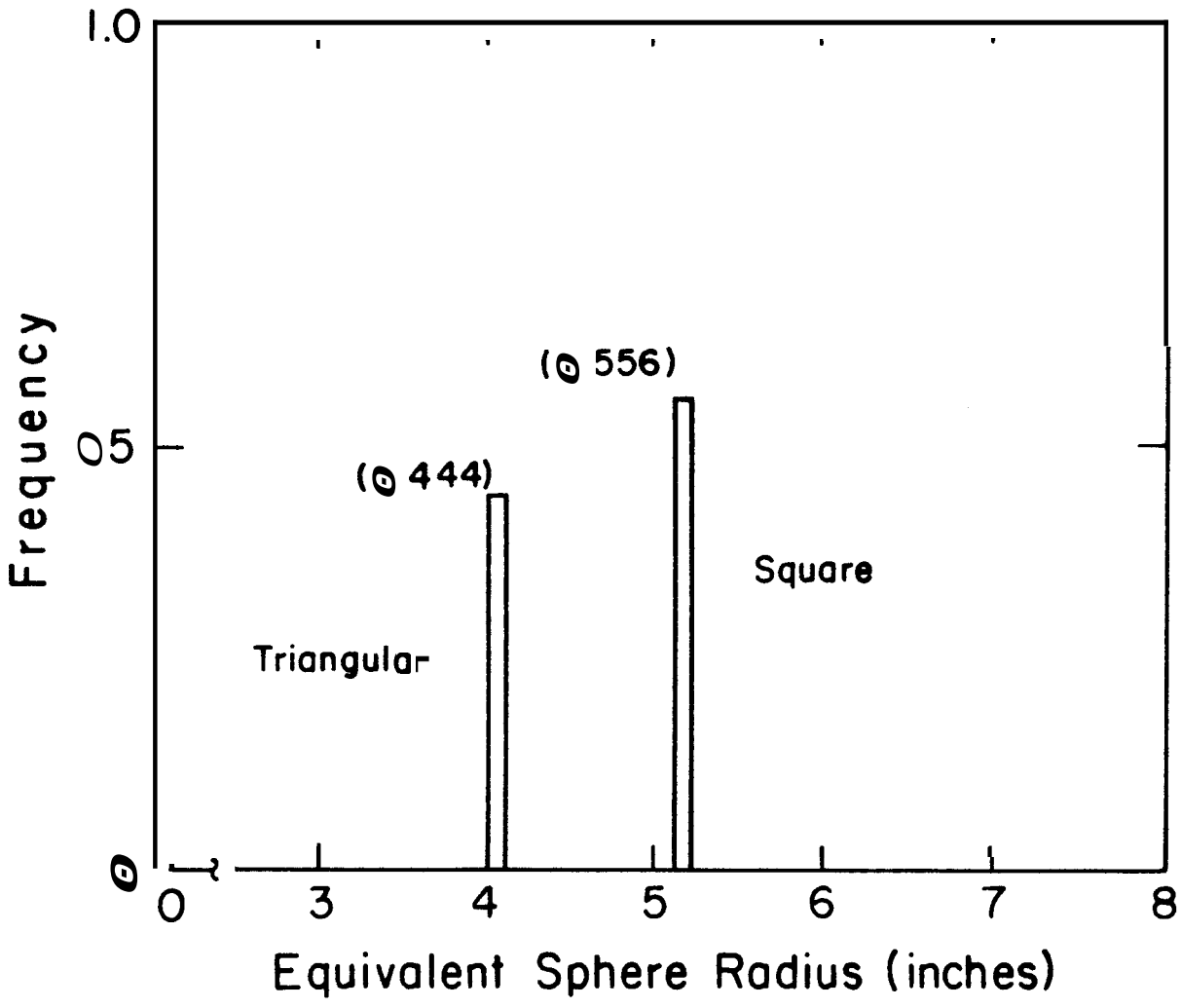

Fig. 3-2: Probability Rock Size Distribution for Regular Shape Rock Loading Used in Experiment 5-2

Table 3-4

CALCULATION OF SUMS FOR
EFFECTIVE ROCK SIZE CALCULATION--
EXPERIMENTAL SYSTEM

j	$p(R_s)$	R_s	$p(R_s)xR_s$	$p(R_s)xR_s^{2/\Psi}K$	$p(R_s)xR_s^3$
1	0.444	4.06	1.803	12.34	29.71
2	0.556	5.12	2.847	18.24	74.63
				30.58	104.34

Using the sums of the last two columns, the equivalent radius for this rock collection calculated from Eq. (2-12) is

$$R_{e,c} = 104.34/30.58 = 3.41 \text{ inch} = 0.284 \text{ ft}$$

C. Physical Properties

Densities for water and rock at the average reservoir temperature during; the production run were obtained from handbooks or other sources. The important thermal properties are specific heat C_r, surface heat transfer coefficient h, thermal conductivity k, and thermal diffusivity a. Values for these parameters were chosen from published sources, except the rock surface heat transfer coefficient h, which based on experiments performed by Kuo et al. (1976), was set at 300 Btu/hr ft^2 °F. Heat transfer from large rock blocks is not very dependent on the surface resistance represented by h for flow of water. Most of the thermal resistance is inside the rock and the value of h selected will not influence results significantly. For laminar

flows over small rock blocks, more accurate value of h as a function of fracture width and flow velocity should be used when available.

Because of the large heat capacity of the steel, values of density ρ_m and specific heat C_m were also required for the steel vessel in the analysis of the experiment. In particular, the heavy flanges near the bottom and at the top of the pressure vessel caused uneven heat transfer along the length of the reservoir and non-uniform cross-sectional temperature distributions and potential natural convection in the water. Although such a perturbation would not be present in the analysis of a geothermal reservoir, it caused an inconsistent calculation with the 1-D analysis of the physical model runs. Moreover, the experimental external heat transfer was not constant with time as assumed in the analysis. Partial resolution of this problem was achieved by lumping the mass of the steel vessel with the rock since the thermal response time of the two are similar. A modified storage ratio that included the effect of the steel was defined as

$$\gamma = \phi/[(C_r^* + C_m^*)(1-\phi)] = \phi/[C^*(1-\phi)] \qquad (3\text{-}1a)$$

where

$$C_r^* = \rho_r C_r/\rho_f C_f \qquad (3\text{-}1b)$$

and

$$C_m^* = \rho_m C_m/\rho_f C_f \qquad (3\text{-}1c)$$

where ρ_m is mass of steel per unit reservoir rock volume. The modified storage ratio is given in Table 3-3.

D. Derived Quantities

The data and formulas needed to calculate the starred quantities in Table 3-3, used as input to the linear heat sweep model, have been described previously. The effective time constant τ of the rock blocks and consequently the heat transfer from the blocks is not affected significantly by the surface heat transfer resistance. This is indicated by the relatively large value of the Biot number for this system which, in effect, is the ratio of internal to surface thermal resistance. Surface heat transfer resistance is expected to be of even less importance in geothermal reservoirs because of the much larger rock sizes and relatively unchanged surface heat transfer coefficient. The number of heat transfer units parameter N_{tu} is strongly dependent on the value of $R_{e,c}$ which in turn is very sensitive to the size of large rock blocks in a given reservoir.

The units of the data in Table 3-3 are in the British system. However, any consistent set of units can be used in the analysis.

3.1.3 Running the Program

The computer program LSWEEP to run the model is given in Appendix A. TO modify the program for a specific problem, changes in input parameters need be made only in the section labeled INITIALIZE CONSTANTS. The pertinent choices, described below, involve the input data for the reservoir, the axial locations at which data are desired, and the specified production times at which output data should be printed.

Input to 1-D Linear Sweep Model. Program

The list of data required to run the 1-D Linear Heat Sweep Model program (LSWEEP) is explained below. (Appendix A gives the input data used for the experimental system problem input.)

NSPACE = Total number of space intervals (integer) assigned to the linear dimension of the problem.

ISPLOC = Axial locations (integers) at which rock and fluid temperatures are to be printed out at the specified production times. In LSWEEP the dimensionless distance from injection point is $x^* = \frac{\text{ISPLOC}}{\text{NSPACE}}$. The number of locations selected, M (integer), should also be specified in the dimension statement given as DIMENSION ISPLOC (M).

NUMLOC = The number of space locations (integer) where data are to be printed out. NUMLOC should be equal to M.

KTIME = Number of time steps (integer) between two consecutive printouts.

NTIME = Total number of time steps (integer) assigned to the run.

TIN = Injected fluid temperature, T_I (°F); TIN is assumed constant in the run.

DT = The temperature difference (°F) between the initial uniform reservoir temperature, T_I, and the injection temperature, T_{in}.

NAI = The initial number (even integer) of coefficients, a_i, in the Stehfest inverse Laplace transform algorithm of the 1-D governing equation. In general, NAI can range from 4 to about 26, depending on the computer accuracy.

NAF = The final number (even integer) of the a_i coefficients chosen for the run. The reservoir heat transfer problem will be computed for number of a_i = NAI, NAI+2, NAI+4, ..., NAF-2, NAF.

XNTU = The number of heat transfer units, N_{tu}, as defined in Eq. (2-3e).

BETA = The recharge temperature parameter β^* specified to fit the inlet region temperature (at $x^* = 0$), as given in Eq. (2-4c).

CS = Heat capacitance ratio, C*, as defined in Table 3-3.

QS = External heat transfer parameter, q^*, as defined in Eq. (2-3f).

F = Reservoir average porosity ϕ.

DELT = Dimensionless time step (as a fraction of residence time t_{re}). For example, NTIME = 100 and DELT = 0.1 will give a 10-residence time calculation. The program listed can compute up to 20 residence times without modifications.

The linear heat sweep model program has been operated on several computers, including the IBM 3081 and VAX II with double precision accuracy. A full analysis with 100 space nodes for 10 residence times consumes roughly 0.3 CPU minutes. The program has also been run on several microcomputers such as the IBM PC and Apple 11. These will need adjustment of the dimensioned time and space parameters to fit the particular available memory space.

Glossary of Output Variables (See Appendix C for the experimental system problem output)

The meaning of those variables which are not self-explanatory is described below:

NA = Number of coefficients a_i in the Stehfest algorithm.

A(I) = The coefficients a_i.

XS = Dimensionless distance from the injection point x^* as given in Eq. (2-3c).

TS = Dimensionless time t^* as in Eq. (2-3d), referenced to the fluid residence time t_{re}.

T = Liquid temperature T_f in degree F at x^* and t^*.

TR = Rock temperaure T_r in degree F at x^* and t^*.

XT = Dimensionless time t^*.

TF(NSPACE,JK) = Produced fluid temperature at $x^* = 1$ and t^*, referenced to initial temperature (T_1) and water injection temperature (T_{in}), i.e., $T_f^*(1, t^*)$. (See Eq. 2-3a)

FP = Reservoir energy recovery fraction F_p.

FC = Reservoir temperature drop fraction F_c.

FE = Reservoir rock energy extracted fraction $F_{E,c}$.

3.1.4 Results

Measured water and rock temperature data for heat extraction experiment 5-2 selected as the experimental system problem are given in Figure 3-3. The thermocouple locations and numbering system were indicated in Figure 3-1. The temperature of the inlet water from the distribution baffle below the rock matrix, indicated by thermocouples IW1 and IW2, is seen to decrease approximately exponentially from temperature levels near the initial matrix temperature to the injection water temperature, indicated by thermocouple 109. The temperature of the water entering the rock matrix at the bottom varied by about 38°C (100°F) from the center to the edge. This relatively large nonuniformity in entering water temperature is probably caused by the high heating rates from the steel vessel lower head and flanges. The inlet temperature used in the 1-D model to simulate the exponential behavior of the inlet temt perature is also shown in Figure 3-3.

The water temperature distribution in the other three measurement planes were quite uniform. The maximum temperature difference between thermocouple readings in a plane was less than 8°C (15°F). The maximum temperature difference is indicated by the vertical bars in Figure 3-3. Water temperatures given for the B-, M-, and T-planes are the average of all thermocouples in each plane. The uncertainty interval of the temperature measurements is estimated to be 3°C (5°F).

The predicted water temperatures as calculated by LSWEEP for the three measurement planes are shown in Figure 3-3 in comparison to the measured values. The predicted water temperatures are always lower than measured in the B- and M-planes while the agreement is quite good in the T-plane. Overall, the agreement between prediction and measurements is good considering the effect of the steel vessel and the many simplifications made in the

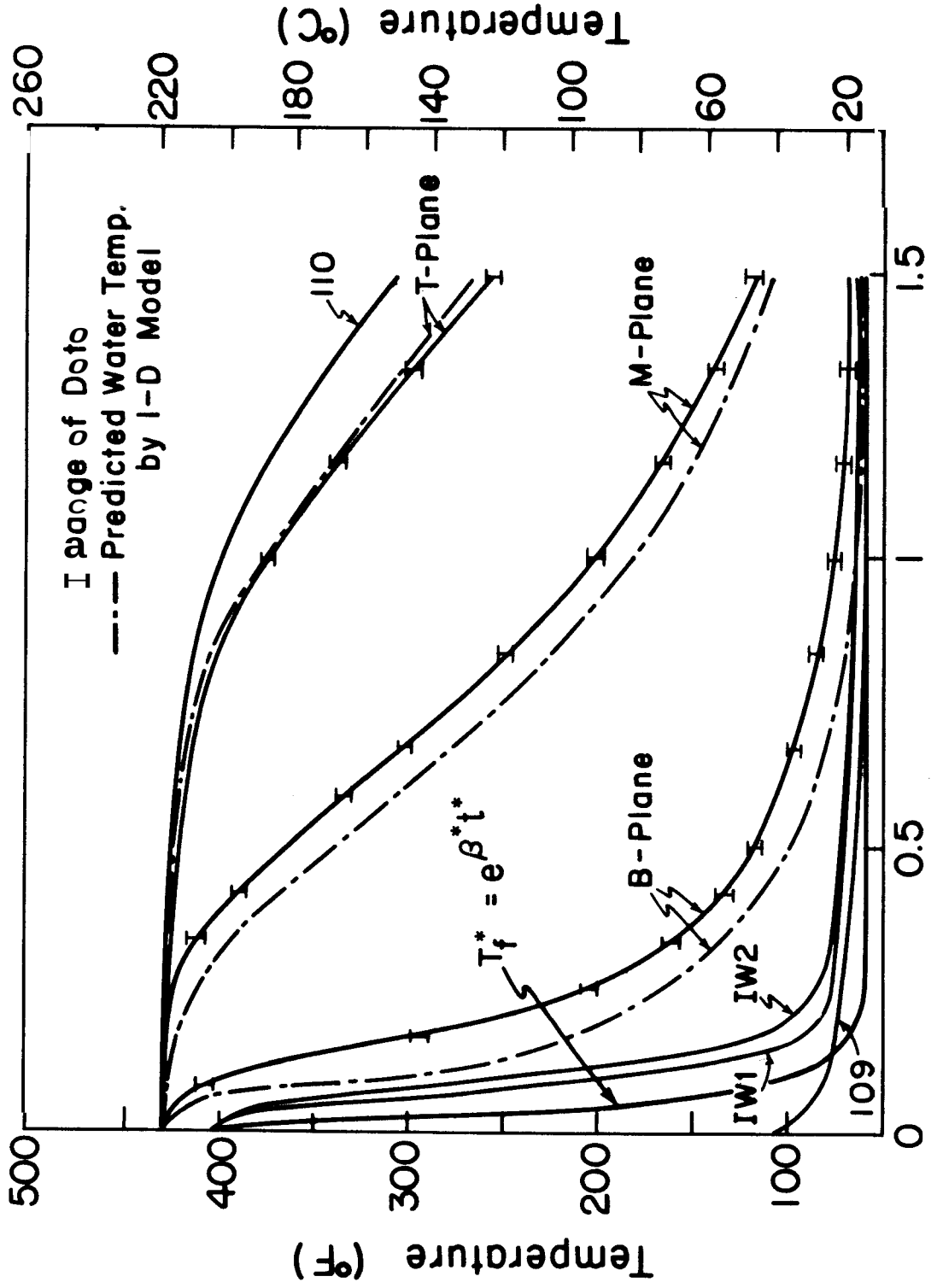

Fig B-3: Comparison of Measured and Predicted Water Temperatures for Experiment 5-2

analysis. Comparison of measured and predicted rock temperatures is not fully meaningful because the rock temperature measurement was performed at the center of rock blocks while the linear heat sweep model calculates the average temperature for the smaller, effective size rock.

The results for the energy extracted fraction $F_{E,c}$*, the energy recovery fraction F_p, and the produced water temperature T_f*(1,t*) are given in Figure *3-4* as functions of non-dimensional time for the experimental system problem. These non-dimensional parameters are computed from the calculated water and rock temperature distributions using typical input values of 100 space intervals (NSPACE = 100) and 0.1 for time step (DELT = 0.1).

The results in Figure *3-4* indicate that energy extracted fraction drops rapidly at early times but recovers significantly at non-dimensional time greater than about one residence time (t* = 1). The physical significance is that the rock sizes are large enough relative to the particular water flow rate to result in incomplete energy extraction from the rock at early times when the rate of change in surrounding water temperature is great. At later times, however, the rate of water temperature change is smaller and the rock cools to a temperature closer to that of the surrounding water. The energy extracted fraction increases at later times.

The thermal fronts in both the rock and water move at approximately the same speed through the reservoir at this relatively low Biot number, but at a much slower speed than the corresponding hydrodynamic front (see Appendix C). A similar phenomenon is also described in Moody's work (1982) at relatively early time temperature modeling in a single-well injection into an infinite fractured non-porous reservoir of negligible rock thermal

*see Section *2.4* for definitions

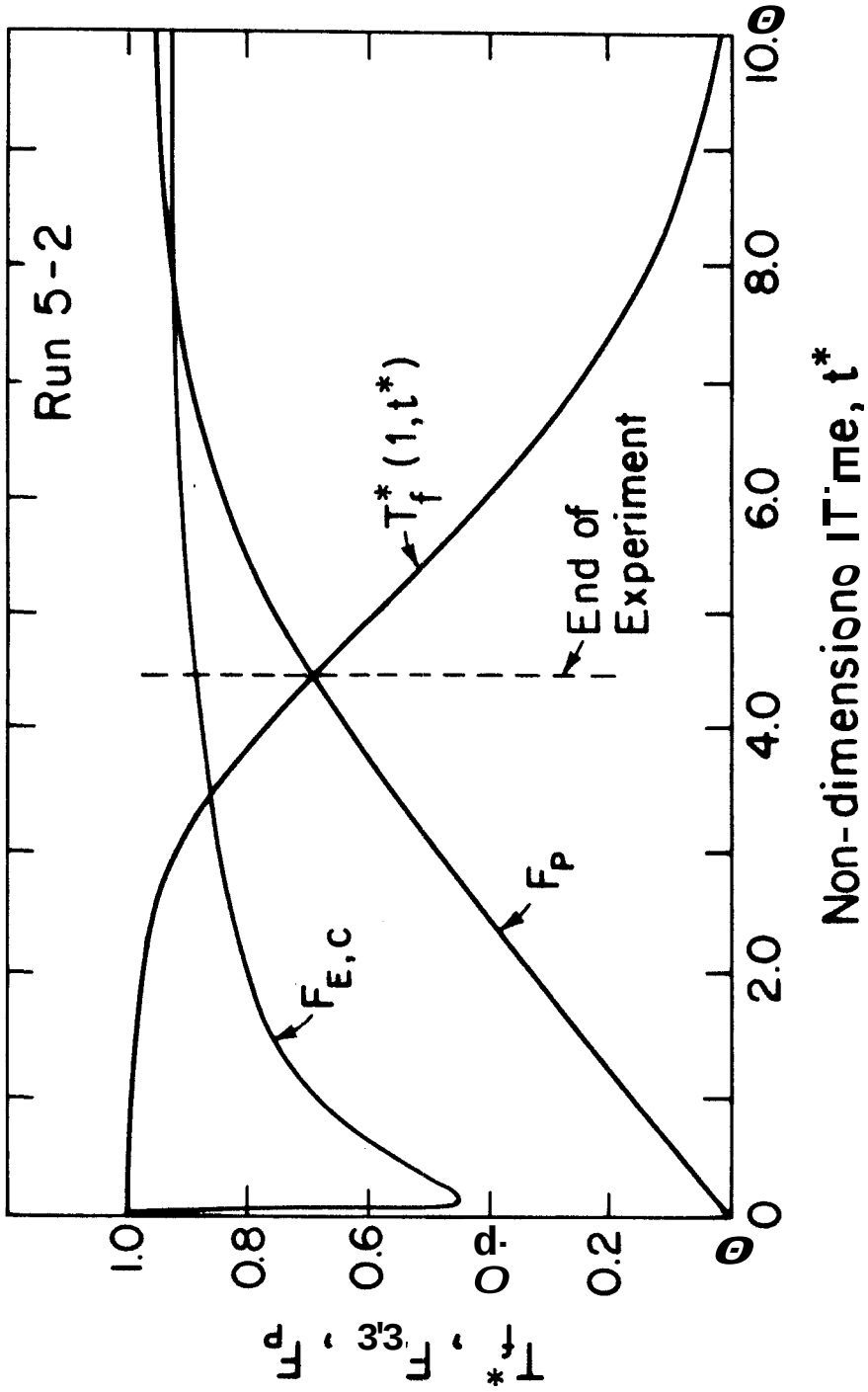

Fig 3-4: Energy Extracted Fraction, Energy Recovery Fraction, and Produced Water Temperature as Functions of Non-dimensional Time for Experiment 5-2

conduction. The thermal breakthrough time is about three times the fluid residence time as shown in Figure 3-4.

The non-dimensional parameter,, defined by Eq. (2-3e), is the number of heat transfer units parameter which is convenient in judging how readily the heat will be extracted from the rock. The smaller this parameter becomes, the harder it is to extract thermal energy, as the reservoir becomes more heat-transfer limited.

3.1.5 Parametric Evaluation of Solution

The Stehfest algorithm used to invert the solution in the Laplace space was described in section 2.3. In using this algorithm, a selection has to be made regarding the number of terms, i.e., the value of NA in the program LSWEEP, to be used in the inversion. A study was made of the sensitivity of solution accuracy to changes in t'he number of terms used in the inversion calculation.

Predicted water temperatures for the B-, M-, and T-planes using *4*, **8**, and *24* terms are compared to the corresponding measured water temperatures in Figure 3-5. The results show that the number of terms has little effect on the solution in the bottom plane while the effect is quite significant in the M- and T-planes when changing from *4* to **8** terms. The effect of changing from **8** to 24 terms is seen to be relatively minor. Similar evaluations performed for three different experimental runs showed essentially the same results as for this run. However, a tendency for the solution to overshoot (oscillate) at the high temperature level and undershoot at the low temperature level was apparent. This tendency is illustrated in Figure 3-5 for the T-plane using 4 terms (the dotted curve) where some overshoot is noted. The oscillatory behavior decreased for ***8*** and 24 terms.

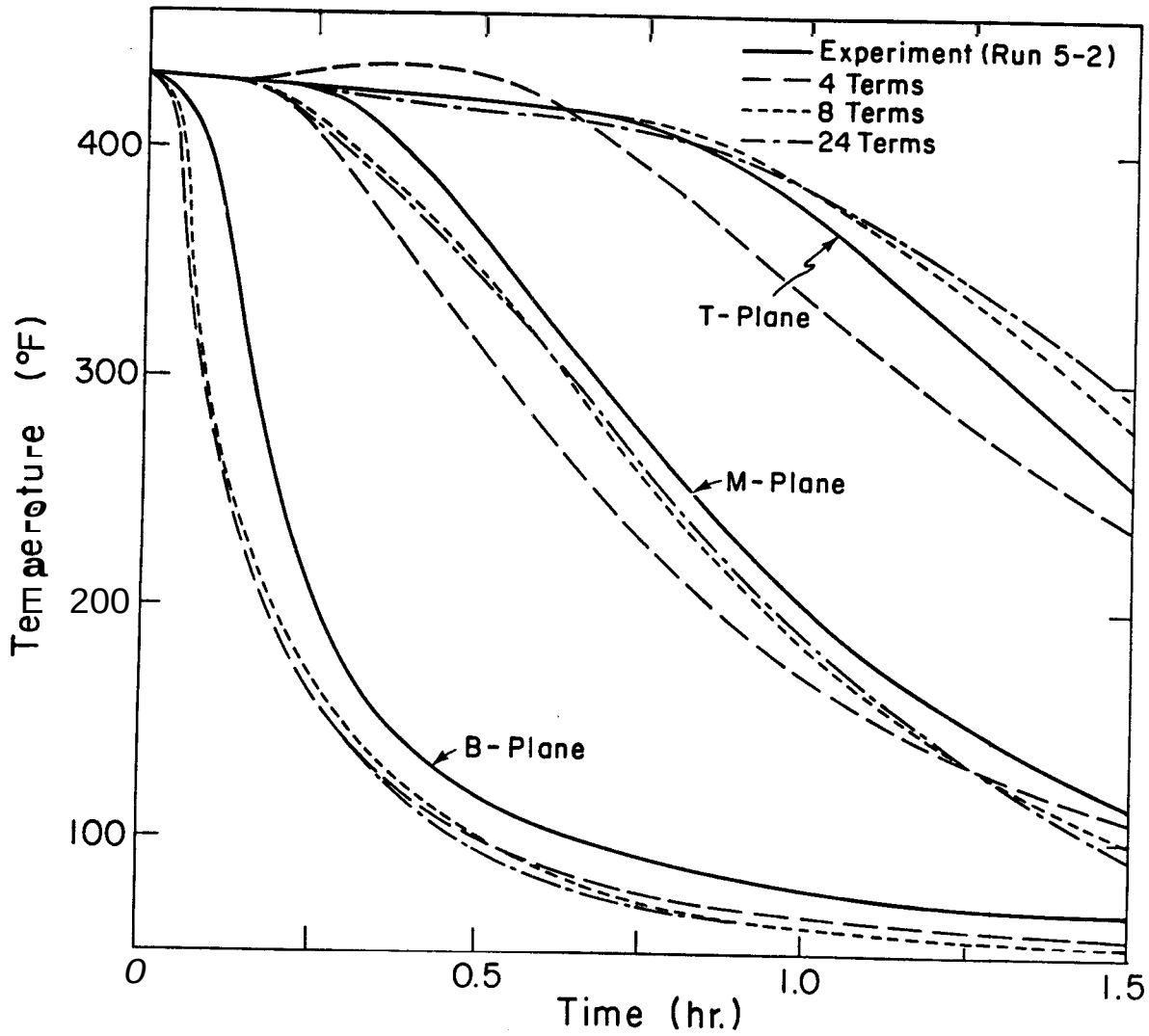

Fig. 3–5: Effect of Number of Terms in the Laplace Inversion Algorithm on the 1-D Model Prediction

The study showed that the solution is subject to some uncertainty. However, the problem can be minimized by using a sufficiently large number of terms. It is recommended that no less than 8 terms (i.e., NA = 8) be used. But the maximum accuracy attainable is limited by the truncation error which also increases as the number of terms used increases. The Stehfest algorithm was also used by Moody (1982) to invert reservoir energy equations, it was found that the inverter is useful for certain time and temperature parameter ranges where analytical solution is non-existent or not well-behaved, but less reliable than analytical solution in general.

3.2 Hypothetical Field Problem

To illustrate the linear heat sweep model for a system without the boundary problems of a physical model, a production run in a hypothetical fractured hydrothermal reservoir is analyzed. A description of the hypothetical field problem, preparation of input data, and results of the model analysis are given in this section.

3.2.1 Problem Description

The hypothetical geothermal reservoir is assumed to consist of a fractured granite rock formation with uniform flow from one side, where natural or injection recharge occurs, to the other side where production occurs. The recharge and production rates are constant and equal throughout the period of time investigated. The pressure in the reservoir is higher than saturation everywhere. The information needed for this analysis is summarized in Table 3-5.

Table 3-5

HYPOTHETICAL FIELD PROBLEM DATA

Reservoir Length, L	3,000 ft
Reservoir Cross-sectional Area, S	3×10^6 ft^2
Average Reservoir Porosity, ϕ	25 percent
Initial Water/Rock Temperature, T_1	550°F
External Heat Transfer, q'	0
Production/Recharge Rate, $\dot{m}_p$	2.10^6 lb_m/hr
Recharge Water Temperature, T_{in}	100°F
Recharge Temperature Parameter, β	$-\infty$ hr^{-1}
Rock Size Distribution	As in Table 3-6

The equivalent sphere rock sizes and the number of each size are given in Table 3-6. This type of information is obtained from well log data on fracture spacing as well as general geologic information available for a given reservoir. The rock block size distribution, calculated from the data in Table 3-6, is presented graphically in Figure 3-6. Calculation of the sums required to determine the effective rock size is illustrated in Table 3-7. Assuming that the average sphericity for the collection of 0.83 (as determined by measurements described in section 2.4), the effective rock block radius is calculated to be

$$R_{e,c} = (0.83)(25,150)/(712.7) = 29.3 \text{ ft}$$

The input data for the hypothetical field problem was prepared following the procedure outlined for the experimental system problem in section 3.1.2. The input data are given in Table 3-8.

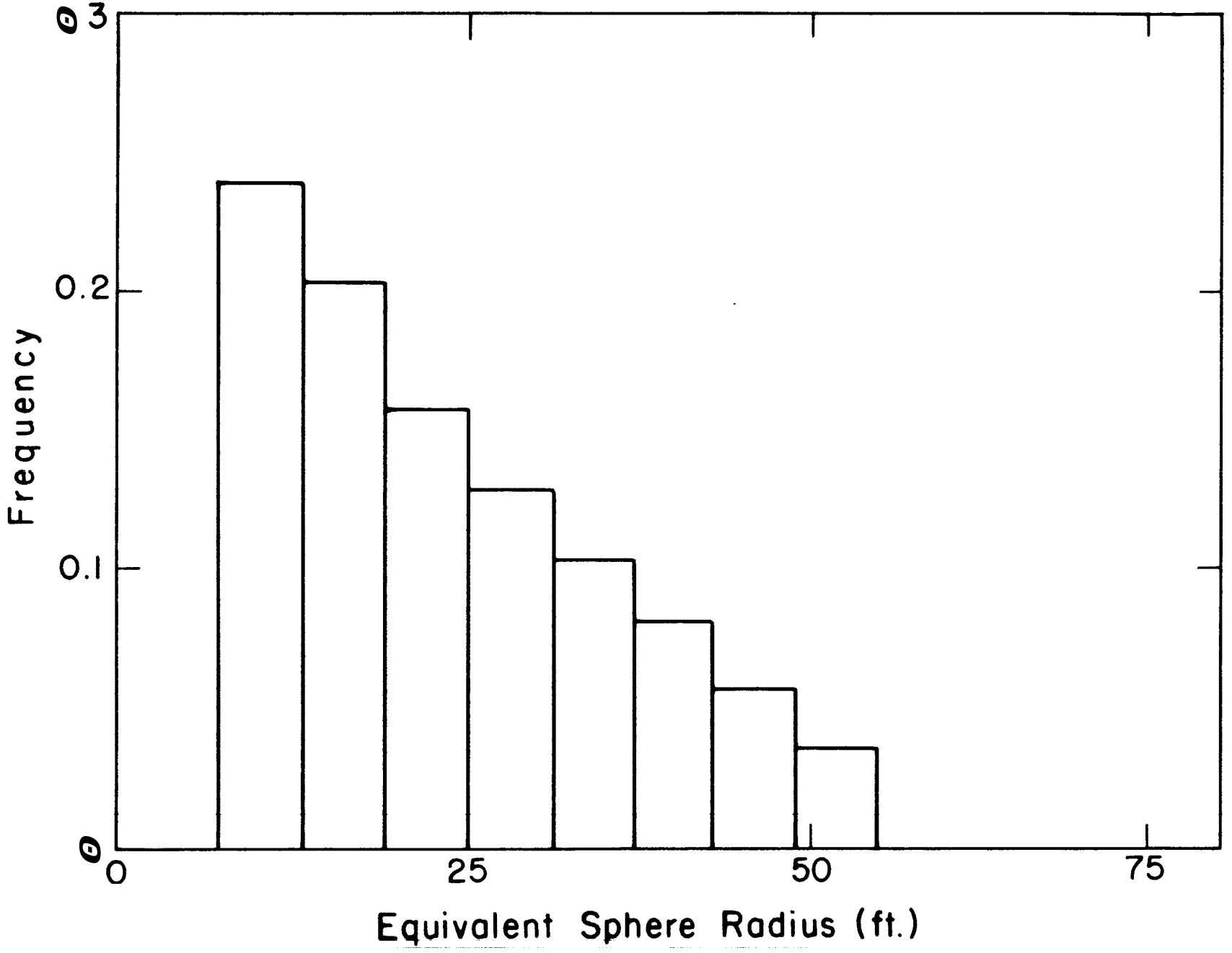

Fig. 3-6: Probability Rock Size Distribution for Hypothetical Field Problem

Table 3–6

HYPOTHETICAL FIELD ROCK SIZE DATA

Rock Size Group	Number of Rocks	Average Equivalent Sphere Rock Radius (ft)
1	100	10
2	85	16
3	65	22
4	54	28
5	43	34
6	32	40
7	24	46
8	15	52

Table 3–7

CALCULATION OF SUMS FOR EFFECTIVE ROCK SIZE CALCULATION-- HYPOTHETICAL FIELD PROBLEM

j	$p(R_s)$	R_s	$p(R_s)xR_s$	$p(R_s)xR_s^2$	$p(R_s)xR_s^3$
1	0.239	10	2.39	23.9	239.0
2	0.203	16	3.25	52.0	831.5
3	0.156	22	3.43	75.5	1661.1
4	0.129	28	3.61	101.1	2831.8
5	0.103	34	3.50	119.1	4048.3
6	0.077	40	3.08	123.2	4928.0
7	0.057	46	2.62	120.6	5548.2
8	0.036	52	1.87	97.3	5061.9
				712.7	25,150

Table 3–8
SUMMARY OF **INPUT** PARAMETERS
TO SWEEP MODEL FOR
HYPOTHETICAL FIELD PROBLEM

	A. Reservoir Conditions	Symbol/Equation	Value	Units
	*Initial Reservoir Temp.	T_1	550	°F
	*Recharge Water Temp.	T_{in}	100	°F
	Recharge Temp. Parameter	β	$-\infty$	hr^{-1}
	Production/Recharge Rate	$\dot{m}_p$	2.0×10^6	lb_m/hr
	External Heat Transfer	q'	0	Btu/ft hr
	B. Geometry Factors			
	*Reservoir Porosity	ϕ	0.25	dim. less
	Reservoir Cross-sectional Area	S	3.0×10^6	ft2
	Reservoir Length	L	3,000	ft
	Effective Rock Radius	$R_{e,c}$	29.3	ft
	Average Rock Sphericity	$\overline{\Psi}_K$	0.83	dim. less
	C. Physical Properties			
	Mean Water Density	ρ_f	57.3	lb_m/ft^3
	Mean Rock Density	ρ_r	167.0	lb_m/ft^3
	Mean Water Specific Heat	C_f	1.03	Btu/lb_m°F
	Mean Rock Specific Heat	C_r	0.22	Btu/lb_m°F
	Rock Surface Heat Trans. Coef.	h	300	Btu/hr°F ft^2
	Rock Thermal Conductivity	k	1.7	Btu/hr°F ft
	Rock Thermal Diffusivity	*a*	0.046	ft^2/hr
	D. Derived Quantities			
	*Rock Capacitance Ratio	$C_r^* = \rho_r C_r / \rho_f C_f$	0.623	dim. less
	Storage Ratio	$\gamma = \phi / C_r^*(1-\phi)$	0.535	dim. less
	Superficial Flow Velocity	$u_f = \dot{m}/\rho_f S$	0.012	ft/hr

Pore Flow Velocity	$w = u_f/\phi$	0.047	ft/hr
Water Residence time	$t_{re} = L/w$	64,463	hr
Rock Biot Number	$N_{Bi} = hR_{e,c}/k$	5,171	dim. less
Effective Rock Time Constant	$\tau = \frac{R_{e,c}^2}{3a}(0.2+1/N_{Bi})$	1,245	hr
*Recharge Temp. Parameter	$\beta^* = \beta t_{re}$	$-\infty$	dim. less
*No. of Heat Transfer Units	$N_{tu} = t_{re}/\tau$	51.8	dim. less
*External Heat Trans. Para.	$q^* = q'L/\dot{m}_p C_f(T_l - T_{in})$	0	dim. less

*starred quantities are inputs to the program

3.2.2 Results

Predicted water and rock temperatures as functions of time at three axial locations in the reservoir are given in Figure 3-7. The calculated energy extraction parameters are given in Figure 3-8. The parameters chosen for this hypothetical field case resulted in a large number of heat transfer units parameter, i.e., 51.8. Thus, the energy extraction from the rock is quite complete indicated by the small rock to water temperature difference at $x^* = 0.5$ in Figure 3-7 and by the high energy extracted fraction ($F_{E,c}$) in Figure 3-8. This fraction is seen to drop to about 0.8 initially before recovering to values close to 1.0 at later times.

The temperature curves in Figure 3-7 exhibit temperature fluctuations at the high and low end of the temperature range. As indicated earlier, this is caused by the Stehfest numerical inversion routine. Thus, temperatures that are higher than the initial value of 550°F and lower than the injection water

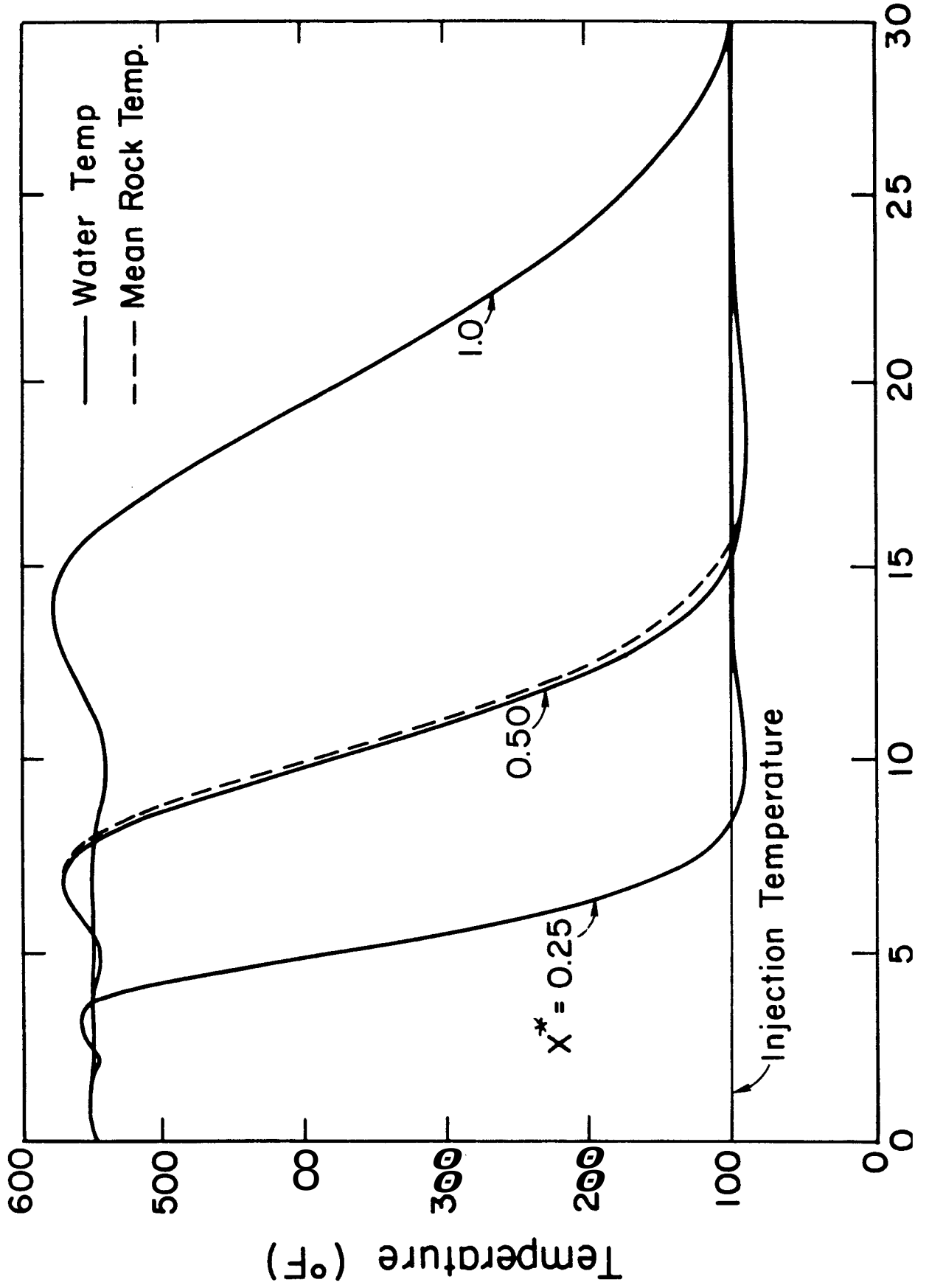

Fig. 3-7: Predicted Water and Rock Temperatures for Hypothetical Field Problem--N_{tu} = 51.8

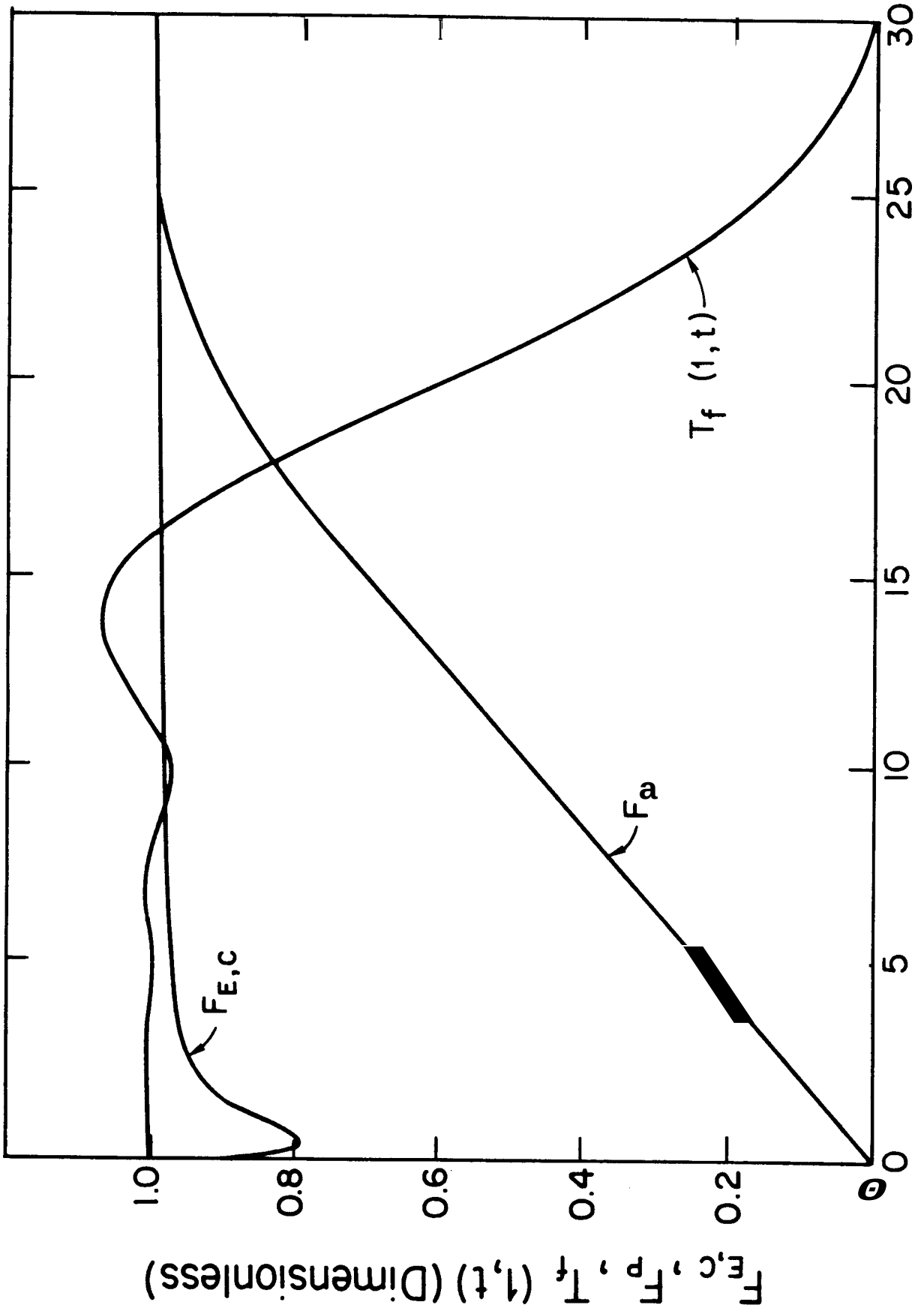

Fig 3-8: Energy Extracted Fraction, Energy Recovery Fraction, and Produced Water Temperature as Functions of Time for Hypothetical Field Problem--N_{tu} = 51.8

temperature of 100°F can be ignored. The temperature fluctuations were evident for all solutions using from 6 to 14 terms. However, a significant trend in water temperature (using 14 terms) at the reservoir exit ($x^* = 1.0$) is evident from Figure 3-7. A major drop in produced water temperature can be expected at production times greater than about 15 years. Economic production from this field would likely stop at about 20 years. At this time the energy recovery fraction (F_P) is seen from Figure 3-8 to be approximately 0.9. Energy production from this reservoir is clearly not rock heat transfer limited.

To illustrate the effect of rock size on the completeness of the energy extraction and on the prediction accuracy of the model, the hypothetical field case was rerun with an effective rock size of four times the original, i.e., 118 ft radius. This resulted in a number of heat transfer units parameter of 3.2. The predicted water temperature and the average rock temperature are given at the same axial positions as for the original case in Figure 3-9. The energy extraction fractions for the calculation are shown in Figure 3-10. The results show that a significant drop in the produced water temperature can be expected at about 10 years as compared to the previous case of 15 years. At this time the energy recovery fraction is seen from Figure 3-10 to be approximately 0.5. Moreover, the temperature fluctuations at the high and low ends of the temperature range did not occur for this case which was also run with 14 terms. Thus, the accuracy of the temperature prediction of the produced fluid appears to improve for lower values of the number of heat transfer units parameter.

Accuracy of the prediction is quite good at lower values of x^* as indicated in the following example. The rock and water temperature at the injection location ($x^* = 0$) where a step change in the water temperature occurs (from T_1 to T_{in} at $t^* = 0^+$) can be solved for analytically.

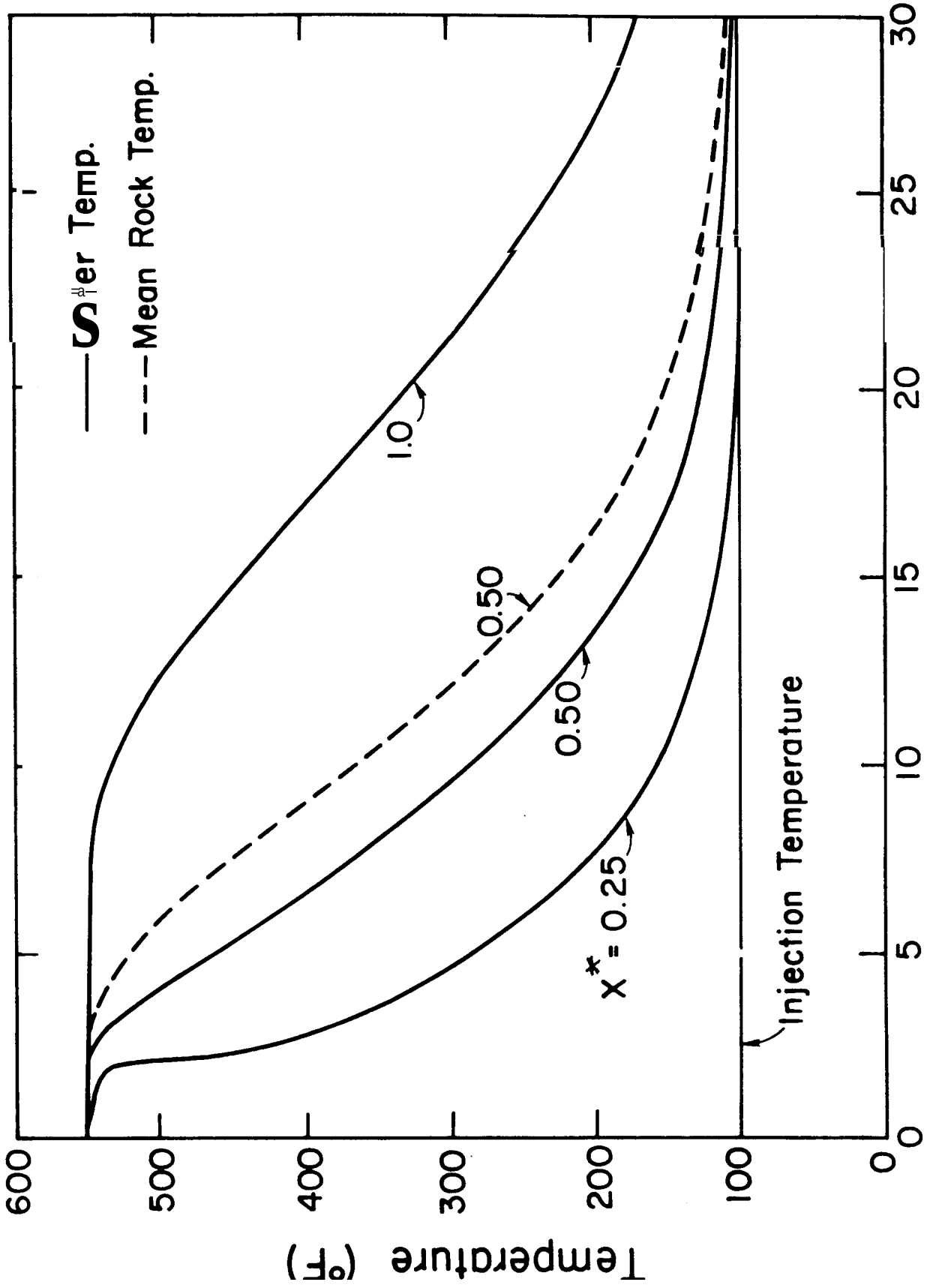

Fig. 3-9: Predicted Water and Rock Temperatures for Hypothetical Field Problem--$N_{t\omega} = 3.2$

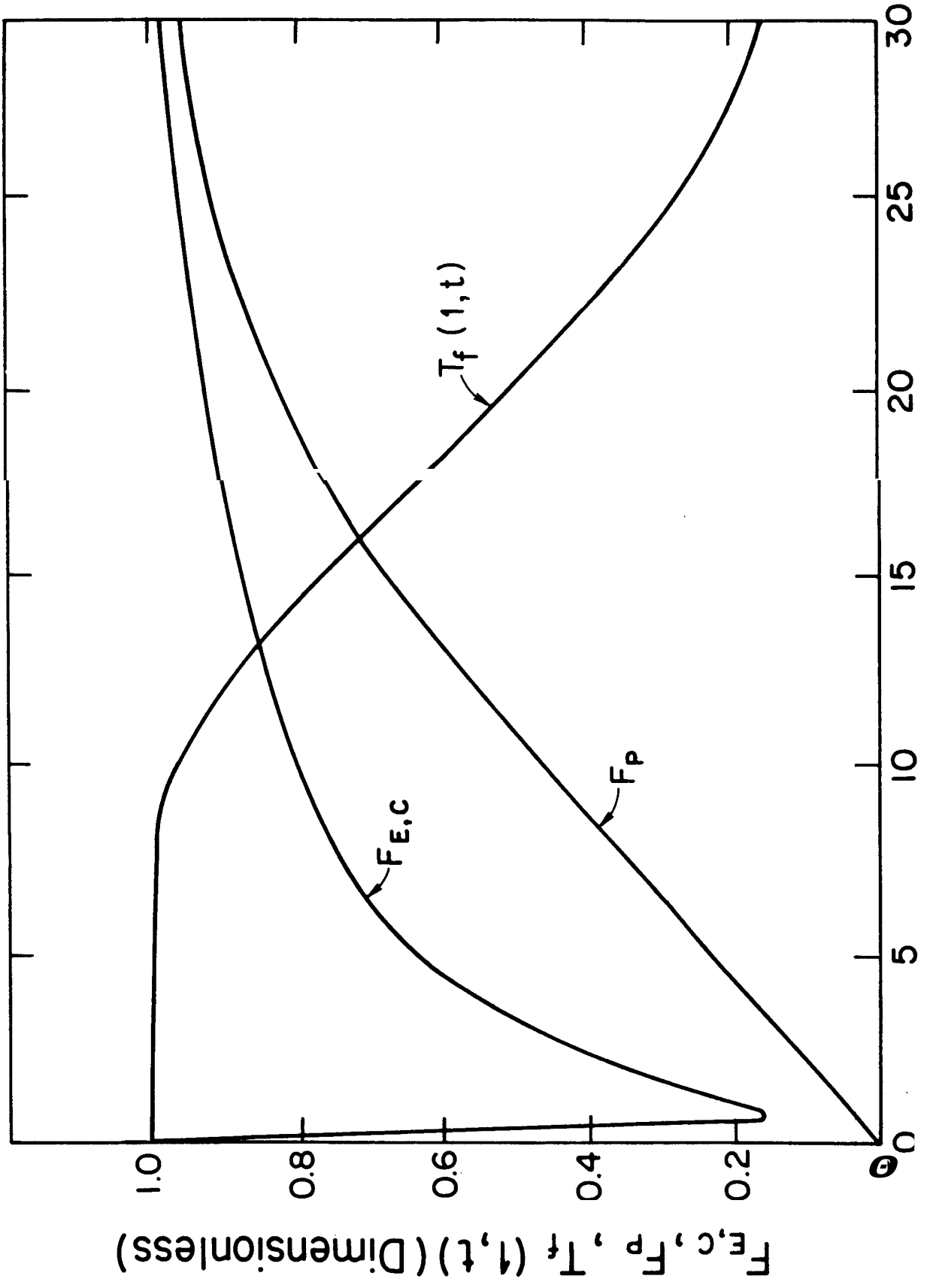

Fig. 3-10: Energy Extracted Fraction, Energy Recovery Fraction, and Produced Water Temperature as Functions of Time for Hypothetical Field Problem--$N_{t_{11}} = 3.2$

Simplification of Eqs. (2-7) gives in this case

$$\hat{T}_f^* = 0 \qquad (3\text{-}2)$$

and $$\hat{T}_r^* = (s + N_{tu})^{-1}$$

Inversion of the Laplace transform gives

$$T_f^* = 0 \qquad (3\text{-}3)$$

and $$T_r^* = e^{-N_{tu}t^*}$$

for $x^* = 0$ at all t^*.

The exponential decrease of the rock temperature from 550°F to the injection temperature of 100°F is given in Figure 3-11. Numerical results obtained from the inversion algorithm are seen to agree closely with the closed-form solution given by Eq. (3-3). The above particular solution to Eq. (2-7) serves to partly verify the numerical inversion procedure used in LSWEEP.

In conclusion, it is cautioned that the present model is not capable of predicting small changes in produced fluid temperature under all conditions. It is useful, however, for evaluating the potential for breakthrough of cold fronts particularly for reservoirs estimated to have high number of heat transfer units.

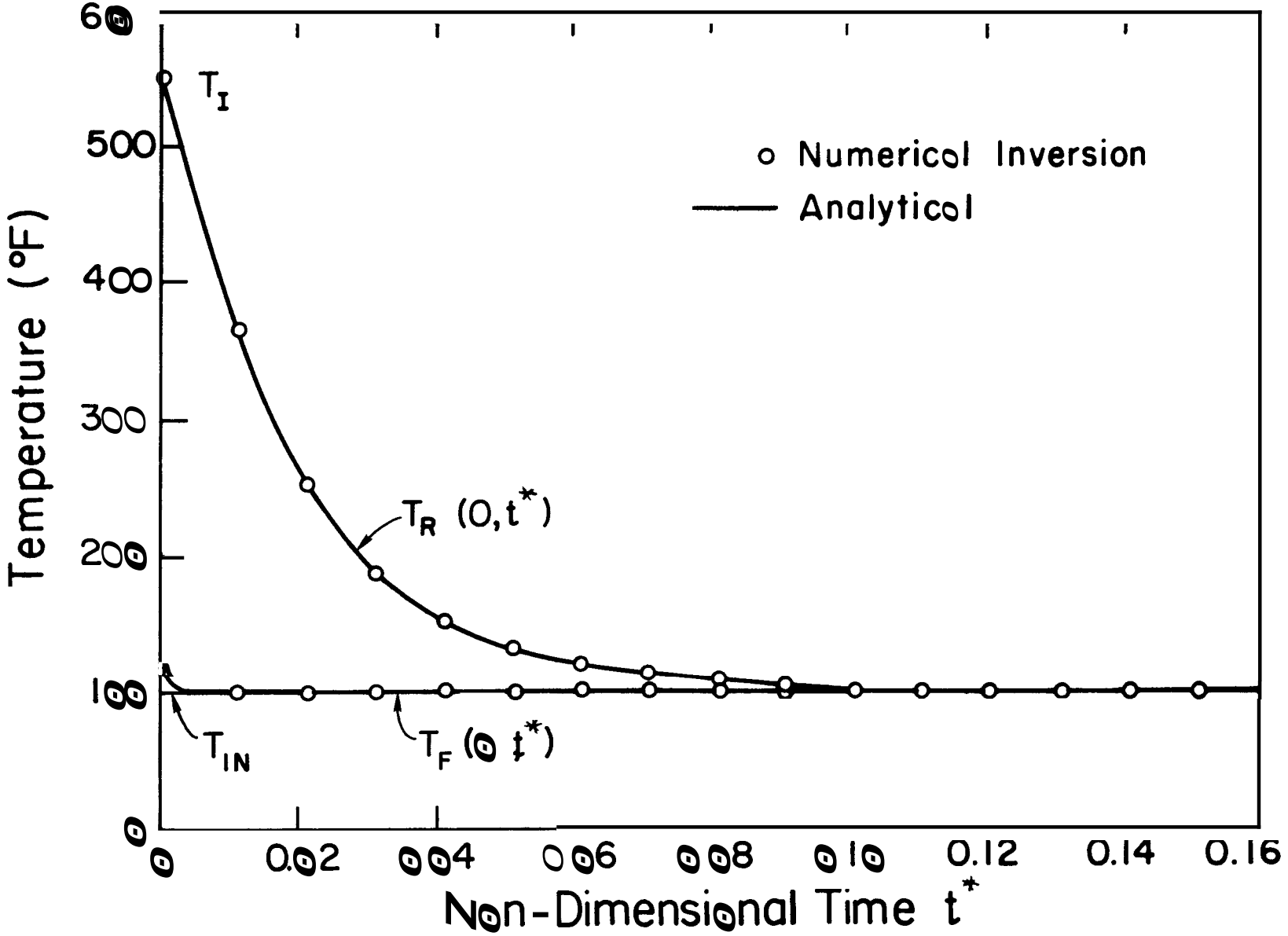

Fig. 3-11: Comparison of Calculated Water and Rock Temperature at X* = 0 from Analytical Solution and Solution Obtained by Numerical Inversion

4. NOMENCLATURE

English Letter Symbols

A = surface area, ft^2

C = specific heat, Btu/lb_m °F

F_E = energy extracted fraction as defined in text, dimensionless

F_c = temperature drop fraction as defined in text, dimensionless

F_p = energy recovery fraction as defined in text, dimensionless

h = heat transfer coefficient, $Btu/hr\ ft^2$ °F

k = thermal conductivity, Btu/hr ft °F

K = parameter defined in text in terms of N_{tu}, γ, and s, dimensionless

L = distance between injection and production wells, ft

$\dot{m}_p$ = produced mass flow rate, lb_m/hr

N = total number of rocks

N_{Bi} = hR/k = Biot number as defined in text, dimensionless

N_L = number of rock groups

N_{tu} = number of heat transfer units parameter defined in text, dimensionless

n_i = number of rock blocks approximately equal size

p = probability

q' = external heat transfer, Btu/ft hr

R = radius, ft

S = cross-sectional area of reservoir, ft^2

s = Laplace space independent variable

t = time, hr

t_{re} = fluid residence time, hr

u = velocity, ft/hr

v = volume, ft3

$w = u/\phi$ = pore flow velocity, ft/hr

x = distance from inlet, ft

Greek Letter Svmbols

α = thermal diffusivity, ft^2/hr

β = recharge temperature parameter, hr^{-1}

γ = storage ratio as defined in text, dimensionless

ρ = density, lb_m/ft^3

σ = standard deviation, ft

τ = time constant, hr

ϕ = porosity of rock matrix, dimensionless

Ψ = sphericity, dimensionless

Subscripts

c = collection

e = effective

f = fluid

in = injection

K = Kuo sphericity

m = metal

r = rock

re = residence

1 = initial value

Special Symbols

$\mathcal{L}^{-1}$ = inverse Laplace transform

$\bar{}$ = mean value

$\hat{}$ = Laplace space variable

$*$ = dimensionless variables defined in text

5. REFERENCES

Hunsbedt, A., Kruger, P., and London, A. L., Laboratory Studies of Stimulated Geothermal Reservoirs, SGP-TR-11, Advanced Technology bept., RANN National Science Foundation, Grant No. NSF-AER-72-03490, December, 1975.

Hunsbedt, A., Kruger, P., and London, A. L., "Recovery of Energy from Fracture-Stimulated Geothermal Reservoirs," Journal of Petroleum Technology, Vol. XXIX, August, 1977, pp. 940-946.

Hunsbedt, A., Kruger, P., and London, A. L., "Laboratory Studies of Fluid Production from Artificially Fractured Geothermal Reservoirs," Journal of Petroleum Technology, Vol. XXX, May, 1978, pp. 712-718.

Iregui, R., Hunsbedt, A., Kruger, P., and London, A. L., Analysis of the Heat Transfer Limitations on the Energy Recovery from Geothermal! Reservoirs, Stanford Geothermal Program Technical Report No. 31, January, 1979.

Kuo, M. T., Kruger, P., and Brigham, W. E., Shape-Factor Correlations for Transient Heat Conduction from Irregular-Shaped Rock Fragments to Surrounding Fluid, Stanford Geothermal Program Technical Report No. 16, June 1976.

Löf, G. O. G. and Hawley, R. W., "Unsteady State Heat Transfer Between Air and Loose Solids," Industrial and Engineering Chemistry, 40, No. 6, June 1948.

Moody, J. D. G., Temperature Transfer in a Convection-Dominant, Naturally Fractured Geothermal Reservoir Undergoing Fluid Injection, Stanford Geothermal Program Technical Report No. 62, June, 1982.

Ramey, H. J., "Wellbore Heat Transmission," Journal of Petroleum Technology,, pp. 427-435, April, 1962.

Ramey, H. J., Kruger, P., and Raghavan, R., "Explosive Stimulation of Hydrothermal Reservoirs," Ch. 13 in P. Kruger and C. Otte, eds., Geothermal Energy, (Stanford University Press, 1973).

Schumann, T. E. W., "Heat Transfer: A Liquid Flowing Through a Porous Prism," Journal of Franklin Institute, September, 1929.

Stehfest, H., "Remark on Algorithm 368 [D5] Numerical Inversion of Laplace Transforms," Communications of the ACM, Vol. 13, No. 10, October, 1970.

Stehfest, H., "Numerical Inversion of Laplace Transforms. Algorithm No. 368," Communications of the ACM, Vol. 13, No. 1, January 1970.

APPENDIX A

1-D LINEAR HEAT SWEEP MODEL PROGRAM LISTING

```
1.      // JOB
2.      // EXEC WATFIV
3.      C
4.      C                              LSWEEP
5.      C
6.      C       PROGRAM TO CALCULATE 1-D LINEAR HEAT SWEEP FLOW
7.      C
8.      C                    I N HYDROTHERHAL RESERVOIR
9.      C
10.     C        ( SUBJECT TO CORRECTIONS BEFORE FINAL RELEASE )
11.     C
12.     C                     FOR  PRODUCTION RUN 5-2
13.     C
14.           INPLICIT REAL*8 (A-H, O-Z)
15.           DIMENSION A(30), T(200), TR(200), TF(100,200), FP(200)
16.           DIMENSION FC(200), TM(200), TN(200), XT(200), FE(200)
17.     C
18.     C INITIALIZE CONSTANTS :
19.     C
20.     C    ISPLOC = SPACE LOCATIONS WHERE DATA ARE TO BE PRINTED
21.     C    NUMLOC = NO. OF SPACE LOCATIONS WHERE DATA ARE TO BE PRINTED
22.     C    KTINE  = NO. OF TIME INTERVALS BETWEEN PRINTOUTS
23.     C    NTIME  = TOTAL TIME INTERVALS
24.     C    NSPACE = TOTAL SPACE INTERVALS
25.     C    TIN    = INJECTION TEMPERATURE (F)
26.     C    DT     = RESERVOIR INITIAL TEMPERATURE - TIN (F)
27.     C    NAI    = INITIAL NUMBER OF COEFFICIENTS A(I)
28.     C    NAF    = FINAL NUMBER OF COEFFICIENTS A(I)
29.     C    XNTU   = HEAT TRANSFER UNITS
30.     C    BETA   = BETA COEFFICIENT
31.     C    CS     = HEAT CAPACITANCE RATIO
32.     C    QS     = EXTERNAL HEAT TRANSFER
33.     C    F      = POROSITY
34.     C    DELT   = TIME STEP
35.     C
36.           DIMENSION ISPLOC(4)
37.           DATA ISPLOC/9,44,93,100/
38.           NUMLOC=4
39.           KTIME=5
40.           NTIME=90
41.           NSPACE=100
42.           TIN = 60.0
43.           DT = 368.0
44.           NAI = 8
45.           NAF = 10
46.           XNTU=2.22
47.           BETA=-7.90
48.           CS=1.016
49.           QS=-0.0524
50.           F=0.173
51.           DELT=0.1
52.     C
53.           SR=F/((1.-F)*CS)
54.           DL2 = DLOG(2.0D00)
55.     C
56.     C DETERMINE NO. OF COEFFICIENT EFFECT I N THE STEHFEST ALSORITHH
57.     C
58.           DO 100 NA=NAI,NAF,2
59.           CALL COEF(NA,A)
60.           PRINT 1004, NA
```

```
      PRINT 1003, (A(I),I=1,NA)
      PRINT 1001, XNTU,CS,SR,F,BETA,QS
C
C EVALUATE FLUID AND ROCK TEMPERATURES
C
      X=0.0
      DO 50 K=1, NSPACE
      X=X+(1.0/NSPACE)
      XS=X
      SUM=0.0
      SUMR=0.0
      Y=0.0
      DO 25 J=1, NTIME
      Y=Y+DELT
      TS=Y
      XT(J)=Y
      SUM=0.
      SUMR=0.
      DO 10 I=1, NA
      S=DL2*DFLOAT( )/TS
      XK=1.0+XNTU*CS*(1.0-F)/(F*(S+XNTU))
      E=(1.0/S+QS/(S*S*XK))-(1.0/S+QS/(S*S*XK)-
     C 1.0/(S-BETA))*DEXP(-XK*XS*S)
      SUM=SUM+A( )*E
   10 SUMR=SUMR+A(I)*(1.0/(S+XNTU)+XNTU/(S+XNTU)*E)
      T(J) = SUM*DL2/TS*DT+TIN
      TF(K,J)=(T(J)-TIN)/DT
      TR(J)=SUMR*DL2/TS*DT+TIN
      DO 15 L=1, NUMLOC
      IF (K .EQ. ISPLOC(L)) GO TO 20
   15 CONTINUE
      GO TO 25
   20 JJJ=MOD(J,KTIME)
      IF (JJJ .NE. 0) GO TO 25
C
C PRINT RESERVOIR TEMPERATURES
C
C XS = LOCATION X
C TS = TIME Y
C T  = FLUID TEMPERATURE (F)
C TR = ROCK TEMPERATURE (F)
C
      PRINT 1002, X, Y, T(J), TR(J)
   25 CONTINUE
   50 CONTINUE
C
C CVALUATE ENERGY FRACTIONS
C
      FPP=0.0
      DO 60 KK=2, NTIME
   60 TM(KK)=(TF(NSPACE,KK)+TF(NSPACE,KK-1))/2.0
      TM(1)=(TF(NSPACE,1)+1.0)/2.0
      DO 65 MM=1, NTIME
      FPP=FPP+DELT*TM(MM)
   65 FP(MM)=FPP*SR/(1.0+SR)
      DO 75 JJ=1,NTIME
      TFF=0.0
      TN(1)=TF(1,JJ)/2.0
      DO 70 II=2,NSPACE
   70 TN(II)=(TF(II,JJ)+TF(II-1,JJ))/2.0
```

```
      DO 72 IJ=1,NSPACE
   72 TFF=TFF+TN(IJ)
      FC(JJ)=1.0-(TFF/DFLOAT(NSPACE))
   75 FE(JJ)=(FP(JJ)/FC(JJ))*(1.0+SR)-SR
C
C PRINT ENERGY FRACTIONS
C
C XT            = TIME
C TF(NSPACE,JK) = PRODUCED FLUID TEMPERATURE
C FP            = RESERVOIR ENERGY FRACTION PRODUCED
C FC            = RESERVOIR TEMPERATURE DROP FRACTION
C FE            = RESERVOIR ROCK ENERGY EXTRACTED FRACTION
C
      PRINT 1006
      PRINT 1005, (XT(JK), TF(NSPACE,JK), FP(JK), FC(JK), FE(JK),
     C  JK=1, NTIME)
  100 CONTINUE
 1001 FORMAT (2X,'HEAT TRANSFER UNITS            = ',F5.2,/,
     C        2X,'HEAT CAPACITANCE RATIO         = ',F5.3,/,
     C        2X,'STORAGE RATIO                  = ',F5.3,/,
     C        2X,'POROSITY                       = ',F5.3,/,
     C        2X,'BETA COEFFICIENT               = ',F6.3,/,
     C        2X,'EXTERNAL HEAT TRANSFER         = ',F7.4,///,
     C  30X,'XS         TS         T(F)      TR(F)'/ )
 1002 FORMAT (28X,F5.2,5X,F5.2,5X,F5.0,5X,F5.0,/)
 1003 FORMAT (10X,E20.10,/)
 1004 FORMAT (///,17X,'NA = ',I3,//,18X,'A(I)',/)
 1005 FORHAT (5(2X, D12.6))
 1006 FORHAT (7X,'XT',12X,'TF',12X,'FP',12X,'FC',12X,'FE')
      STOP
      END
C
      SUBROUTINE COEF (NA,A)
C
C DETERMINE THE COEFFICIENTS A(I) I N THE STEHFEST ALGORITHM
C
      IMPLICIT REAL*8 (A-H, O-Z)
      DIMENSION A(30),G(31),H(30)
      G(1)=1.0
      NH=NA/2
      DO 10 I=1,NA
   10 G(I+1)=G( [illegible]
      H(1)=2./G(NH)
      DO 30 I=2,NH
   30 H( [illegible]=I**NH*G(2*I+1)/(G(NH-I+1)*G(I+1)*G(I))
      SN=2*(NH-NH/2*2)-1
      DO 60 I=1,NA
      A(I)=0.
      K1=(I+1)/2
      K2=I
      IF(K2 .GT. NH) K2=NH
      DO 40 K=K1,K2
   40 A(I)=A(I)+H(K)/(G(I-K+1)*G(2*K-I+1))
      A(I)=SN*A(I)
   60 SN=-SN
      RETURN
      END
$DATA
```

APPENDIX B

FLOW DIAGRAM FOR 1-D LINEAR HEAT SWEEP MODEL PROGRAM

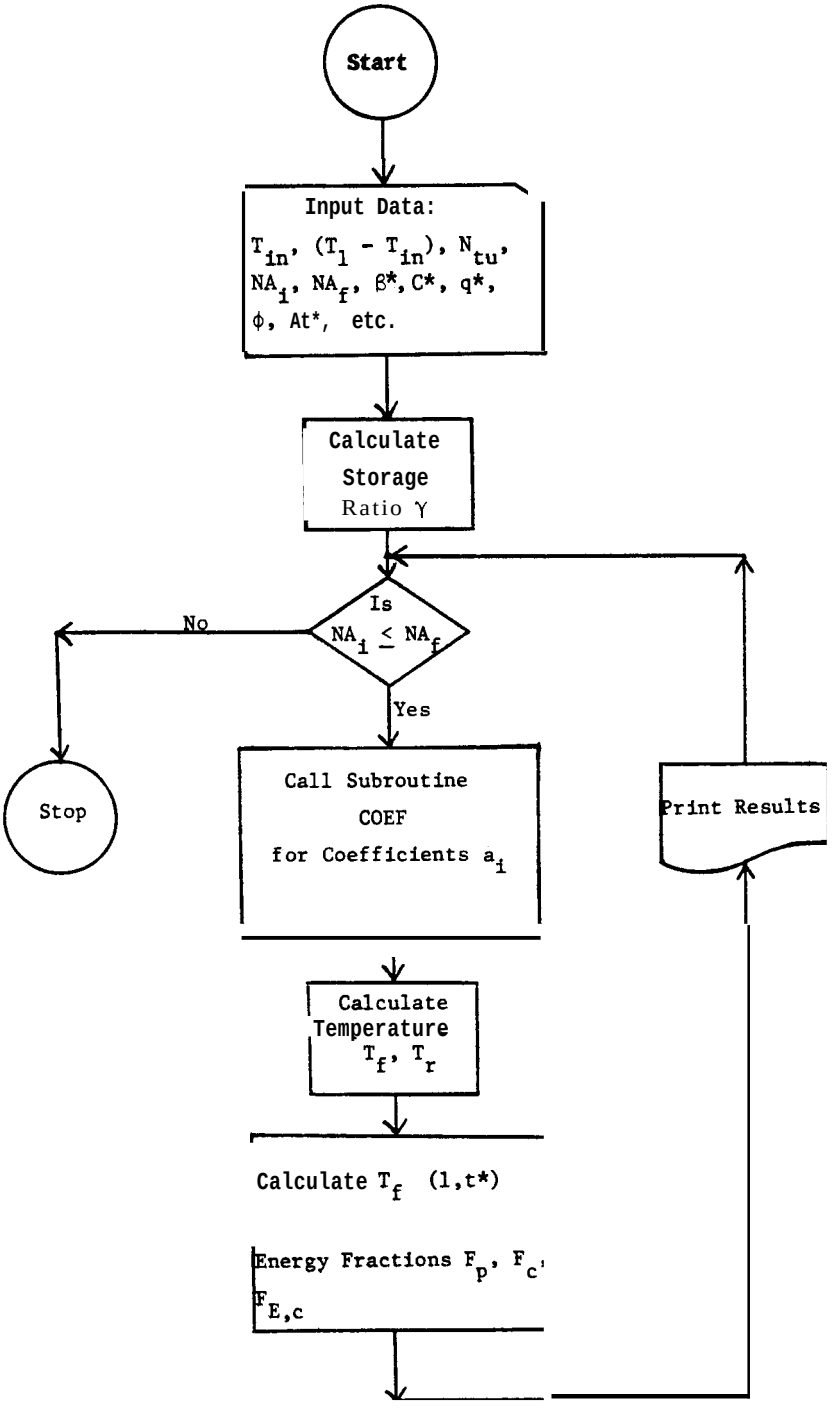

APPENDIX C

EXPERIMENTAL SYSTEM PROBLEM OUTPUT

NA = 8

A(I)

-0.3333333333D 00

0.4833333333D 02

-0.9060000000D 03

0.5464666667D 04

-0.14376666670 05

0.1873000000D 05

-0.11946666670 05

0.2986666667D 04

HEAT TRANSFER UNITS	= 2.22
HEAT CAPACITANCE RATIO	= 1.016
STORAGE RATIO	= 0.206
POROSITY	= 0.173
BETA COEFFICIENT	= -7.900
EXTERNAL HEAT TRANSFER	= -0.0524

XS	TS	T(F)	TR(F)
0.09	0.50	221.	342.
0.09	1.00	136.	223.
0.09	1.50	96.	148.
0.09	2.00	77.	106.
0.09	2.50	67.	03.
0.09	3.00	62.	71.
0.09	3.50	60.	64.
0.09	4.00	59.	61.
0.09	4.50	58.	59.
0.09	5.00	58.	58.
0.09	5.50	58.	58.
0.09	6.00	58.	57.
0.09	6.50	58.	57.
0.09	7.00	58.	57.
0.09	7.50	58.	58.
0.09	8.00	58.	58.
0.09	8.50	58.	58.
0.09	9.00	58.	58.

0.44	0.50	423.	426.
0.44	1.00	397.	416.
0.44	1.50	347.	385.
0.44	2.00	287.	334.
0.44	2.50	230.	277.
0.44	3.00	182.	225.
0.44	3.50	145.	181.
0.44	4.00	117.	147.
0.44	4.50	97.	120.
0.44	5.00	83.	100.
0.44	5.50	72.	85.
0.44	6.00	65.	75.
0.44	6.50	60.	67.
0.44	7.00	56.	61.
0.44	7.50	54.	57.
0.44	8.00	52.	54.
0.44	8.50	51.	52.
0.44	9.00	50.	51.
0.93	0.50	425.	427.
0.93	1.00	423.	424.
0.93	1.50	422.	424.
0.93	2.00	420.	424.
0.93	2.50	409.	419.
0.93	3.00	386.	404.
0.93	3.50	354.	378.
0.93	4.00	317.	345.
0.93	4.50	279.	309.
0.93	5.00	243.	273.
0.93	5.50	210.	238.
0.93	6.00	180.	207.
0.93	6.50	155.	179.
0.93	7.00	133.	155.

0.93	7.50	115.	134.
0.93	8.00	100.	117.
0.93	8.50	88.	102.
0.93	9.00	78.	90.
1.00	0.50	425.	427.
1.00	1.00	423.	424.
1.00	1.50	422.	423.
1.00	2.00	422.	424.
1.00	2.50	416.	423.
1.00	3.00	400.	413.
1.00	3.50	373.	392.
1.00	4.00	340.	364.
1.00	4.50	304.	331.
1.00	5.00	268.	296.
1.00	5.50	234.	262.
1.00	6.00	203.	230.
1.00	6.50	176.	201.
1.00	7.00	152.	175.
1.00	7.50	131.	152.
1.00	8.00	114.	132.
1.00	8.50	100.	116.
1.00	9.00	88.	102.

XT	TF	FP	FC	FE
0.1000000D 00	0.996672D 00	0.170457D-01	0.277722D-01	0.534244D 00
0.2000000 00	0.99513013 00	0.340498D-01	0.604376D-01	0.47349111 00
0.300000D 00	0.994082D 00	0.51 0318D-01	0.880890D-01	0.492704D 00
0.400000D 00	0.993153D 00	0.679969D-01	0.111246D 00	0.531187D 00
0.500000D 00	0.992174D 00	0.849457D-01	0.131823D 00	0.57117513 00
0.600000D 00	0.9910510 00	0.101877D 00	0.1510280 00	0.607549D 00
0.700000D 00	0.989756D 00	0.118787D 00	0.169489D 00	0.639258D 00
0.800000D 00	0.988343D 00	0.1356740 00	0.187523D 00	0.666577D 00
0.900000D 00	0.986924D 00	0.15253713 00	0.205290D 00	0.690123D 00
0.100000D 01	0.985638D 00	0.169377D 00	0.222881D 00	0.710514D 00
0.110000D 01	0.984612D 00	0.186197D 00	0.240358D 00	0.728270D 00
0.120000D 01	0.983936D 00	0.2030020 00	0.2577661) 00	0.743800D 00
0.130000D 01	0.983644D 00	0.219800D 00	0.275148D 00	0.757424D 00
0.140000D 01	0.983706D 00	0.236595D 00	0.292537D 00	0.769394D 00
0.150000D 01	0.984041D 00	0.2533940 00	0.3099638 00	0.779920D 00
0.160000D 01	0.984521D 00	0.2701390 00	0.327446D 00	0.789176D 00
0.170000D 01	0.984986D 00	0.287013D 00	0.344999D 00	0.797320D 00

0.180000D 01	0.985256D 00	0.3038330 00	0.362625D 00	0.804491D 00
0.190000D 01	0.9851490 00	0.3206550 00	0.380320D 00	0.810817D 00
0.200000D 01	0.9844870 00	0.3374700 00	0.398072D 00	0.816415D 00
0.210000D 01	0.9831061) 00	0.354267D 00	0.41586113 00	0.8213920 00
0.220000D 01	0.9808610 00	0.371033D 00	0.4336648 00	0.8258420 00
0.230000D 01	0.977635D 00	0.3877530 00	0.451451D 00	0.829854D 00
0.240000D 01	0.973331D 00	0.404409D 00	0.469190D 00	0.8335000 00
0.250000D 01	0.967884D 00	0.420981D 00	0.486849D 00	0.836849D 00
0.260000D 01	0.961249D 00	0.437450D 00	0.504392D 00	0.839956D 00
0.2700000 01	0.953409D 00	0.4537958 00	0.52178513 00	0.842870D 00
0.280000D 01	0.9443660 00	0.469997D 00	0.538994D 00	0.845631D 00
0.290000D 01	0.934143D 00	0.486034D 00	0.555989D 00	0.848272D 00
0.300000D 01	0.922777D 00	0.50188613 00	0.572739D 00	0.850821D 00
0.310000D 01	0.910318D 00	0.5175368 00	0.589216D 00	0.853299D 00
0.320000D 01	0.8968310 00	0.532963D 00	0.605395D 00	0.855723D 00
0.3300000 01	0.8823840 00	0.548152D 00	0.621254D 00	0.858106D 00
0.340000D 01	0.867054D 00	0.563088D 00	0.636773D 00	0.860458D 00
0.3500000 01	0.850923D 00	0.577754D 00	0.651935D 00	0.862786D 00
0.360000D 01	0.834072D 00	0.5921391) 00	0.666727D 00	0.865094D 00
0.370000D 01	0.816586D 00	0.606231D 00	0.681136D 00	0.867386D 00
0.380000D 01	0.7985470 00	0.620019D 00	0.6951540 00	0.869662D 00
0.3900000 01	0.780038D 00	0.633495D 00	0.708774D 00	0.871923D 00
0.400000D 01	0.761138D 00	0.646653D 00	0.7219900 00	0.874168D 00
0.410000D 01	0.741922D 00	0.659484D 00	0.734801D 00	0.876396D 00
0.420000D 01	0.722465D 00	0.6713860 00	0.747206D 00	0.878604D 00
0.4300000 01	0.702833D 00	0.684154D 00	0.759205D 00	0.8807900 00
0.440000D 01	0.6830931) 00	0.695985D 00	0.770801D 00	0.882953D 00
0.450000D 01	0.663303D 00	0.707480D 00	0.781998D 00	0.885088D 00
0.4600000 01	0.6435200 00	0.7186360 00	0.792799D 00	0.8671930 00
0.470000D 01	0.623795D 00	0.729455D 00	0.803212D 00	0.889266D 00
0.480000D 01	0.604174D 00	0.7399380 00	0.8132421) 00	0.891303D 00
0.490000D 01	0.5847010 00	0.750088D 00	0.822897D 00	0.893303D 00
0.500000D 01	0.5654130 00	0.759906D 00	0.832185D 00	0.895262D 00
0.5100000 01	0.546346D 00	0.769397D 00	0.841115D 00	0.89717913 00
0.520000D 01	0.527529D 00	0.778565D 00	0.8496950 00	0.8990521) 00
0.530000D 01	0.508990D 00	0.787414D 00	0.857935D 00	0.90087813 00
0.540000D 01	0.490753D 00	0.795949D 00	0.865843D 00	0.902655D 00
0.550000D 01	0.472839D 00	0.804175D 00	0.873431D 00	0.904382D 00
0.5600000 01	0.4552640 00	0.8120980 00	0.880707D 00	0.906058D 00
0.570000D 01	0.4380430 00	0.819724D 00	0.887682D 00	0.907681D 00
0.580000D 01	0.421190D 00	0.827060D 00	0.8943650 00	0.9092500 00
0.590000D 01	0.404714D 00	0.834111D 00	0.900767D 00	0.910765D 00
0.6000000 01	0.38862213 00	0.840883D 00	0.9068960 00	0.912224D 00
0.610000D 01	0.372922D 00	0.8473850 00	0.912762D 00	0.913626D 00
0.620000D 01	0.357617D 00	0.853621D 00	0.9183760 00	0.914973D 00
0.6300000 01	0.342709D 00	0.8596001) 00	0.923745D 00	0.9162620 00
0.640000D 01	0.328199D 00	0.865328D 00	0.928880D 00	0.917494D 00
0.650000D 01	0.314088D 00	0.870811D 00	0.933790D 00	0.918669D 00
0.6600000 01	0.300375D 00	0.8760560 00	0.938482D 00	0.919786D 00
0.670000D 01	0.287055D 00	0.8810710 00	0.9429660 00	0.9208470 00
0.680000D 01	0.274127D 00	0.8858621) 00	0.947250D 00	0.9218500 00
0.690000D 01	0.2615860 00	0.890436D 00	0.951342D 00	0.922797D 00
0.700000D 01	0.249427D 00	0.894798D 00	0.955249D 00	0.923687D 00
0.710000D 01	0.2376440 00	0.898956D 00	0.958980D 00	0.9245220 00
0.720000D 01	0.2262320 00	0.902916D 00	0.962541D 00	0.9253011) 00
0.730000D 01	0.215185D 00	0.906685D 00	0.9659390 00	0.926026D 00
0.740000D 01	0.20449413 00	0.910268D 00	0.969182D 00	0.926696D 00
0.750000D 01	0.194153D 00	0.913671D 00	0.972276D 00	0.927314D 00
0.760000D 01	0.184155D 00	0.916901D 00	0.97522711 00	0.927878D 00
0.770000D 01	0.174491D 00	0.919962D 00	0.9780410 00	0.928390D 00
0.7800000 01	0.1651540 00	0.9228620 00	0.9807250 00	0.9288520 00
0.790000D 01	0.156136D 00	0.925605D 00	0.983284D 00	0.929263D 00
0.800000D 01	0.147429D 00	0.928196D 00	0.9857230 00	0.929624D 00
0.810000D 01	0.139024D 00	0.930642D 00	0.988047D 00	0.929937D 00
0.820000D 01	0.1309140 00	0.932946D 00	0.99026313 00	0.930203D 00
0.830000D 01	0.1230901) 00	0.935115D 00	0.99237313 00	0.930422D 00
0.8400000 01	0.115545D 00	0.937152D 00	0.994384D 00	0.93059413 00
0.850000D 01	0.108270D 00	0.939063D 00	0.996299D 00	0.930723D 00
0.860000D 01	0.101257D 00	0.9408510 00	0.998123D 00	0.930807D 00
0.870000D 01	0.944993D-01	0.942523D 00	0.9998600 00	0.930848D 00
0.880000D 01	0.879880D-01	0.944080D 00	0.100151D 01	0.930847D 00
0.890000D 01	0.817158D-01	0.9455290 00	0.100309D 01	0.930805D 00
0.900000D 01	0.756752D-01	0.946873D 00	0.100458D 01	0.9307230 00

NA = 10

A(I)

0.8333333333D-01

-0.3208333333D 02

0.1279000000D 04

-0.1562366667D 05

0.8424416667D 05

-0.2369575000D 06

0.3759116667D 06

-0.3400716667D 06

0.1640625000D 06

-0.3281250000D 05

HEAT TRANSFER WITS = 2.22
HEAT CAPACITANCE RATIO = 1.016
STORAGE RATIO = 0.206
POROSITY = 0.173

BETA COEFFICIENT = -7.900
EXTERNAL HEAT TRANSFER = -0.0524

XS	TS	T(F)	TR(F)
0.09	0.50	221.	342.
0.09	1.00	137.	224.
0.09	1.50	96.	148.
0.09	2.00	76.	105.
0.09	2.50	66.	02.
0.09	3.00	62.	69.
0.09	3.50	60.	63.
0.09	4.00	59.	60.
0.09	4.50	58.	59.
0.09	5.00	58.	58.
0.09	5.50	58.	58.
0.09	6.00	58.	58.
0.09	6.50	58.	58.
0.09	7.00	58.	58.
0.09	7.50	58.	58.

0.09	8.00	58.	58.
0.09	8.50	58.	58.
0.09	9.00	58.	58.
0.44	0.50	423.	426.
0.44	1.00	3%.	415.
0.44	1.50	348.	385.
0.44	2.00	290.	337.
0.44	2.50	233.	282.
0.44	3.00	183.	228.
0.44	3.50	144.	182.
0.44	4.00	115.	145.
0.44	4.50	94.	117.
0.44	5.00	79.	96.
0.44	5.50	69.	81.
0.44	6.00	62.	71.
0.44	6.50	57.	63.
0.44	7.00	54.	58.
0.44	7.50	52.	55.
0.44	8.00	51.	53.
0.44	8.50	51.	51.
0.44	9.00	50.	50.
0.93	0.50	425.	427.
0.93	1.00	423.	425.
0.93	1.50	421.	423.
0.93	2.00	417.	421.
0.93	2.50	407.	416.
0.93	3.00	389.	404.
0.93	3.50	360.	382.
0.93	4.00	325.	353.
0.93	4.50	287.	318.
0.93	5.00	249.	281.
0.93	5.50	213.	244.
0.93	6.00	181.	210.

0.93	6.50	153.	180.
0.93	7.00	130.	153.
0.93	7.50	110.	130.
0.93	8.00	94.	111.
0.93	8.50	81.	96.
0.93	9.00	71.	83.
1.00	0.50	425.	427.
1.00	1.00	423.	425.
1.00	1.50	421.	423.
1.00	2.00	419.	421.
1.00	2.50	413.	419.
1.00	3.00	400.	411.
1.00	3.50	378.	395.
1.00	4.00	348.	371.
1.00	4.50	312.	340.
1.00	5.00	276.	306.
1.00	5.50	240.	270.
1.00	6.00	206.	236.
1.00	6.50	176.	204.
1.00	7.00	150.	175.
1.00	7.50	128.	150.
1.00	8.00	109.	128.
1.00	8.50	94.	110.
1.00	9.00	81.	95.

XT	TF	FP	FC	FE
0.100000D 00	0.9966741) 00	0.170457D-01	0.277276D-01	0.535436D 00
0.200000D 00	0.995117D 00	0.340497D-01	0.603055D-01	0.4749770 00
0.300000D 00	0.994044D 00	0.510312D-01	0.881385D-01	0.4923050 00
0.400000D 00	0.993112D 00	0.679957D-01	0.111402D 00	0.530136D 00
0.500000D 00	0.992227D 00	0.849446D-01	0.131969D 00	0.570305D 00
0.600000D 00	0.991356D 00	0.101879D 00	0.1511200 00	0.607067D 00
0.700000D 00	0.99046313 00	0.118797D 00	0.169553D 00	0.639014D 00
0.800000D 00	0.989512D 00	0.135701D 00	0.187622D 00	0.666287D 00
0.900000D 00	0.988475D 00	0.152587D 00	0.205497D 00	0.689511D 00
0.100000D 01	0.987342D 00	0.169454D 00	0.223259D 00	0.7093820 00
0.110000D 01	0.98612913 00	0.186302D 00	0.240944D 00	0.7265220 00
0.120000D 01	0.984866D 00	0.20312813 00	0.258568D 00	0.741445D 00
0.130000D 01	0.983590D 00	0.219933D 00	0.276138D 00	0.7545540 00
0.1400000 01	0.982334D 00	0.236716D 00	0.2936600 00	0.766165D 00
0.150000D 01	0.9811140 00	0.253478D 00	0.311140D 00	0.776520D 00
0.1600000 01	0.9799250 00	0.2702200 00	0.3285830 00	0.785807D 00
0.170000D 01	0.978736D 00	0.286941D 00	0.345997D 00	0.794173D 00
0.180000D 01	0.977493D 00	0.303641D 00	0.363386D 00	0.8017390 00
0.190000D 01	0.9761190 00	0.3203190 00	0.380752D 00	0.808602D 00

0.200000D 01	0.974518D 00	0.336972D 00	0.398096D 00	0.814846D 00
0.210000D 01	0.972585D 00	0.353595D 00	0.4154160 00	0.820542D 00
0.220000D 01	0.970209D 00	0.370180D 00	0.432703D 00	0.82575613 00
0.230000D 01	0.967278D 00	0.3867210 00	0.449949D 00	0.830543D 00
0.240000D 01	0.963686D 00	0.403205D 00	0.467140D 00	0.834957D 00
0.250000D 01	0.959337D 00	0.419622D 00	0.484259D 00	0.839043D 00
0.260000D 01	0.9541450 00	0.435958D 00	0.501287D 00	0.842844D 00
0.270000D 01	0.948041D 00	0.452197D 00	0.518204D 00	0.846398D 00
0.280000D 01	0.940972D 00	0.468323D 00	0.534986D 00	0.849738D 00
0.290000D 01	0.932899D 00	0.484321D 00	0.551611D 00	0.852895D 00
0.300000D 01	0.923802D 00	0.5001720 00	0.568055D 00	0.855894D 00
0.310000D 01	0.913676D 00	0.515858D 00	0.584295D 00	0.858758D 00
0.320000D 01	0.902529D 00	0.531363D 00	0.600307D 00	0.861506D 00
0.3300000 01	0.8903840 00	0.5466691) 00	0.6160700 00	0.864156D 00
0.340000D 01	0.877276D 00	0.561760D 00	0.631563D 00	0.866720D 00
0.350000D 01	0.863247D 00	0.5766190 00	0.646766D 00	0.869210D 00
0.360000D 01	0.8483500 00	0.591231D 00	0.66166313 00	0.871636D 00
0.370000D 01	0.832645D 00	0.605582D 00	0.676237D 00	0.874004D 00
0.380000D 01	0.816196D 00	0.619658D 00	0.690475D 00	0.876320D 00
0.390000D 01	0.799072D 00	0.6334470 00	0.7043640 00	0.878589D 00
0.400000D 01	0.781342D 00	0.646939D 00	0.717894D 00	0.880813D 00
0.410000D 01	0.763080D 00	0.6601240 00	0.7310570 00	0.8829940 00
0.4200000 01	0.7443560 00	0.6729931) 00	0.743847D 00	0.885134D 00
0.430000D 01	0.725243D 00	0.685539D 00	0.75625913 00	0.887233D 00
0.440000D 01	0.705812D 00	0.697756D 00	0.768290D 00	0.889292D 00
0.450000D 01	0.686130D 00	0.709639D 00	0.779938D 00	0.891308D 00
0.460000D 01	0.6662620 00	0.721185D 00	0.7912030 00	0.893283D 00
0.470000D 01	0.646273D 00	0.7323900 00	0.802087D 00	0.8952150 00
0.480000D 01	0.626220D 00	0.743253D 00	0.8125911) 00	0.897102D 00
0.490000D 01	0.606160D 00	0.7537740 00	0.8227208 00	0.898943D 00
0.500000D 01	0.586145D 00	0.763953D 00	0.832478D 00	0.900737D 00
0.510000D 01	0.5662230 00	0.773791D 00	0.8418700 00	0.9024830 00
0.520000D 01	0.5464400 00	0.783290D 00	0.850903D 00	0.904179D 00
0.530000D 01	0.526835D 00	0.7924520 00	0.859583D 00	0.905823D 00
0.540000D 01	0.507447D 00	0.8012820 00	0.867918D 00	0.907415D 00
0.550000D 01	0.488309D 00	0.809783D 00	0.875915D 00	0.908954D 00
0.560000D 01	0.46945013 00	0.817959D 00	0.883583D 00	0.910438D 00
0.570000D 01	0.450899D 00	0.825816D 00	0.890931D 00	0.911866D 00
0.580000D 01	0.4326770 00	0.833359D 00	0.897967D 00	0.913237D 00
0.590000D 01	0.414806D 00	0.840594D 00	0.904700D 00	0.914552D 00
0.6000000 01	0.3973030 00	0.84752713 00	0.911140D 00	0.915808D 00
0.610000D 01	0.3801840 00	0.854165D 00	0.917296D 00	0.9170060 00
0.620000D 01	0.363460D 00	0.860513D 00	0.923177D 00	0.918146D 00
0.6300000 01	0.347142D 00	0.866580D 00	0.928792D 00	0.919226D 00
0.640000D 01	0.331238D 00	0.872371D 00	0.934151D 00	0.9202480 00
0.650000D 01	0.315753D 00	0.877894D 00	0.9392630 00	0.921210D 00
0.660000D 01	0.300692D 00	0.883157D 00	0.944137D 00	0.922114D 00
0.670000D 01	0.286057D 00	0.8881660 00	0.948782D 00	0.922958D 00
0.6800000 01	0.2718480 00	0.892929D 00	0.953206D 00	0.9237441) 00
0.690000D 01	0.258066D 00	0.897453D 00	0.957418D 00	0.92447213 00
0.700000D 01	0.244708D 00	0.9017450 00	0.961427D 00	0.925143D 00
0.710000D 01	0.231772D 00	0.905813D 00	0.965240D 00	0.925756D 00
0.720000D 01	0.219254D 00	0.9096630 00	0.968867D 00	0.926312D 00
0.730000D 01	0.207148D 00	0.913303D 00	0.9723140 00	0.926813D 00
0.740000D 01	0.195450D 00	0.916740D 00	0.975589D 00	0.927259D 00
0.750000D 01	0.184153D 00	0.919981D 00	0.978700D 00	0.927650D 00
0.760000D 01	0.173249D 00	0.92303213 00	0.981654D 00	0.927987D 00
0.770000D 01	0.162733D 00	0.9259018 00	0.984457D 00	0.928272D 00
0.780000D 01	0.152596D 00	0.928593D 00	0.987116D 00	0.928506D 00
0.790000D 01	0.142830D 00	0.931115D 00	0.989638D 00	0.928688D 00
0.800000D 01	0.133425D 00	0.933473D 00	0.992029D 00	0.928821D 00
0.810000D 01	0.124375D 00	0.935674D 00	0.994294D 00	0.928905D 00
0.820000D 01	0.1156700 00	0.937723D 00	0.996440D 00	0.928941D 00
0.830000D 01	0.107300D 00	0.939627D 00	0.998472D 00	0.928930D 00
0.8400000 01	0.992565D-01	0.94139013 00	0.100040D 01	0.928874D 00
0.850000D 01	0.915308D-01	0.9430191) 00	0.10022213 01	0.928773D 00
0.860000D 01	0.8411340-01	0.944518D 00	0.100394D 01	0.928629D 00
0.870000D 01	0.769950D-01	0.945894D 00	0.1005561) 01	0.928442D 00
0.880000D 01	0.701666D-01	0.9471500 00	0.100710D 01	0.928214D 00
0.890000D 01	0.636191D-01	0.948292D 00	0.100855D 01	0.9279471) 00